A MIXED H^1-CONFORMING FINITE ELEMENT METHOD FOR SOLVING MAXWELL'S EQUATIONS WITH NON-H^1 SOLUTION[*]

HUO-YUAN DUAN[†], ROGER C. E. TAN[‡], SUH-YUH YANG[§], AND CHENG-SHU YOU[¶]

Abstract. In this paper, we propose and analyze a mixed H^1-conforming finite element method for solving Maxwell's equations in terms of electric field and Lagrange multiplier, where the multiplier is introduced accounting for the divergence constraint. We mainly focus on the case that the physical domain is non-convex and its boundary includes reentrant corners or edges, which may lead the solution of Maxwell's equations to be a non-H^1 very weak function and thus causes many numerical difficulties. The proposed method is formulated in the stabilized form by adding an additional mesh-dependent stabilization term to the mixed variational formulation. A general framework of stability and error analysis is established. Specifically, a pair of H^1-conforming finite elements, namely the CP_2-P_1 elements, for electric field and multiplier is studied and its stability and error bounds are also derived. Numerical experiments for source problems as well as eigenvalue problems on the L-shaped and cracked domains are presented to illustrate the high performance of the proposed mixed H^1-conforming finite element method.

Key words. Maxwell's equations, non-H^1 very weak solution, H^1-conforming finite element method, coercivity, Babuška-Brezzi inf-sup condition, error estimates, C^1 elements

AMS subject classifications. 65N30, 65N15, 65N25, 35Q61, 35J47

1. Introduction. As is well-known, the solution of Maxwell's equations would be an H^1 function when the physical domain is convex polygonal or smooth enough. In such case, the usual H^1-conforming finite element method (FEM) based on the plain curl/div formulation is effective and efficient [45, 46], just like the Poisson equation of Laplacian whose methods and theory are classical and well established (cf. [20, 21]). This gives rise to a question: how about the case of non-H^1 solution? Unfortunately, the H^1-conforming FEM would fail for solving Maxwell's equations whenever the exact solution is a non-H^1 function [13]. Such a non-H^1 solution, which is very singular, may take place if, for example, the physical domain is a non-convex polygon with some reentrant corners and/or edges [2, 26, 27]. The reason behind the failure is due to the fact that the density in the norm $\| \cdot \|_{0,\mathrm{curl,div}}$ would not hold for the H^1-conforming finite element space in the solution space $H_0(\mathrm{curl};\Omega) \cap H(\mathrm{div};\Omega)$ (cf. [28, 43]). This therefore leads the finite element solutions to an incorrect convergence. That is, it does not converge to the true solution in the non-H^1 space, but to a member of H^1 space instead. However, it is quite a natural choice to use the H^1-conforming finite elements, because the space $H_0(\mathrm{curl};\Omega) \cap H(\mathrm{div};\Omega)$ is a physically and mathematically meaningful choice for the solution of Maxwell's equations and any $H_0(\mathrm{curl};\Omega) \cap H(\mathrm{div};\Omega)$-conforming finite elements of polynomials must necessarily belong to the H^1 space, and consequently continuous in the entire domain. To sum up, we use the classical H^1-conforming FEM to solve Maxwell's equations when the solution is an H^1 function. When the solution is non-H^1, it would be still desirable to consider the H^1-conforming method using nodal-continuous Lagrange elements, since there are numerous algorithms, softwares and solution methods available, and also as an interesting alternative to the edge element methods [44, 58].

Only over the last decade, several successful methods for numerically solving Maxwell's equations with non-H^1 solutions have been proposed and analyzed, see e.g., [7, 11, 14, 15, 18, 28, 32, 34, 35, 36, 37, 38, 54, 55]. One can find that the central idea behind these methods is to modify the plain curl/div formulation in either the continuous stage or the discrete stage. In this paper, we shall develop a new mixed H^1-conforming FEM for Maxwell's equations in the vector potential form. We mainly focus on the case that the physical domain is non-convex and its boundary includes reentrant corners or edges, which may lead the solution of Maxwell's equations to be a non-H^1 very weak function. The proposed method is based on a Galerkin variational formulation which is the same as the one that is typically employed in the edge element methods [58]. It is a mixed or saddle-point form, involving the electric field and the Lagrange multiplier. The multiplier is introduced to weaken the divergence constraint. Such a constraint is usually expressed as divergence-free, also called gauge condition [13, 45], for the uniqueness of the solution. The divergence constraint corresponds to the physical law of conservation of some quantity such as charge. The main difference with the edge element methods is that we use the H^1-conforming finite element space for electric field, instead of the edge elements which are $H(\mathrm{curl}; \Omega)$-conforming only. Moreover, a mesh-dependent term of the divergence operator is additionally added to the mixed variational formulation for the sake of stability. The mesh-dependent stabilization term is element-by-element defined, and also well-defined even in the case of edge element. For this newly proposed FEM, the stability is analyzed in the framework of classical theory for saddle-point problems, see, e.g., [17]. In other words, by the verification of the $\mathcal{K}_h$-coercivity and the Babuška-Brezzi inf-sup condition, we can show that the method is stable.

For this proposed method, we find that if the solution of electric field is smooth enough, optimal error bounds can follow from the classical theory of saddle-point problems [17]. On the other hand, when the solution of electric field is non-H^1, we will analyze in detail a specific pair of H^1-conforming mixed finite elements, namely the CP_2-P_1 elements. The Lagrange multiplier is approximated by linear (P_1) elements and the electric field is solved by CP_2 elements, where CP_2 means the space of composite quadratic (P_2) elements so that it contains the gradient of a kind of C^1 elements. Other composite elements in two and three dimensions can be constructed in order that the gradient of C^1 elements can be included as a subspace, while the composite triangulations of C^1 elements and the finite element interpolation properties have been now readily available in two and three dimensions, see [4, 5, 47, 48, 49, 50, 51, 52, 53]. In this paper, we first provide a general framework of stability and error analysis and then give further error estimates for the CP_2-P_1 finite element space. These finite elements and their analysis of stability and error bounds are new to Maxwell's equations, to the authors' knowledge. In order to illustrate the high performance of the proposed mixed H^1-conforming FEM, we present several numerical examples for source problems as well as eigenvalue problems on L-shaped and cracked non-convex domains. Numerical results confirm the theoretical analysis.

The remainder of this paper is organized as follows. In Section 2, the system of Maxwell's equations is introduced, together with its variational formulation. The mixed H^1-conforming FEM is proposed in Section 3, where an additional mesh-dependent stabilization term is added into the variational formulation. A general framework of stability and error analysis is provided in Section 4. Error estimates of the CP_2-P_1 finite element space are established in Section 5. Numerical results of the source and eigenvalue problems on non-convex domains are presented in Section 6. Some concluding remarks are given in Section 7.

2. Maxwell's equations and the mixed variational formulation. Let Ω be a non-convex polygonal domain in $\mathbb{R}^2$ with Lipschitz boundary Γ having reentrant corners or edges. The $L^2(\Omega)$ function space is defined as

$$L^2(\Omega) = \left\{ q : \Omega \to \mathbb{R} \text{ is Lebesgue measurable with } \int_\Omega q^2 < \infty \right\},$$

equipped with the L^2 inner product $(p,q) := \int_\Omega pq$ and the L^2 norm $\|q\|_0 := \sqrt{(q,q)}$. The vector L^2 space, $(L^2(\Omega))^2$, will denote the product of two $L^2(\Omega)$ spaces. The corresponding L^2 inner product and the L^2 norm will be denoted by the same notations $(\cdot,\cdot)$ and $\|\cdot\|_0$, i.e., $(u,v) = \int_\Omega u \cdot v$ and $\|v\|_0 = \sqrt{(v,v)}$.

In this paper, we will focus on the following boundary value problem for Maxwell's equations: find the electric field $u = (u_1, u_2)^\top$ such that

$$\mathbf{curl}\,\mathrm{curl}\,u = f, \quad \mathrm{div}\,u = g \quad \text{in } \Omega, \quad u \cdot \tau = 0 \quad \text{on } \Gamma, \tag{2.1}$$

where $f \in (L^2(\Omega))^2$ and $g \in L^2(\Omega)$ are given source terms and τ denotes the unit tangential vector along boundary Γ. We define the curl operator on the vector-valued function $v = (v_1, v_2)$ by $\mathrm{curl}\,v := \partial_x v_2 - \partial_y v_1$ and on a scalar function φ by $\mathbf{curl}\,\varphi := (\partial_y \varphi, -\partial_x \varphi)$. We also define the divergence operator on v as $\mathrm{div}\,v := \partial_x v_1 + \partial_y v_2$. This type of Maxwell's equations which takes a simplest form is usually referred to as the vector potential equations [19, 40, 41]. The divergence equation $\mathrm{div}\,u = g$ in Ω, also called gauge condition in engineering community, is often introduced as a constraint with $g = 0$ to ensure the uniqueness of the vector potential u.

We can consider the more general Maxwell equations in the form

$$\mathbf{curl}\,\mathrm{curl}\,u + \lambda u = f, \quad \mathrm{div}\,u = g \quad \text{in } \Omega, \quad u \cdot \tau = 0 \quad \text{on } \Gamma, \tag{2.2}$$

where $g = \mathrm{div}\,f / \lambda$ for $\lambda \neq 0$. Here λ may stand for the inverse of the time step in the time-discretization of transient Maxwell's equations [25, 58]. If (2.1) is numerically solved well with the FEM, one should expect that (2.2) can also be well solved from the same method in the case of $\lambda > 0$. Furthermore, we may also consider the Maxwell eigenvalue problem by setting f and g to zero in (2.2) and letting $(u, -\lambda)$ be the unknown eigenfunction and eigenvalue. The numerical results presented in Section 6 below show that the Maxwell eigenvalue problem can be efficiently solved by our method (described in Section 3). However, a further theory still needs to be investigated, since the eigenvalue problem may be quite different from the source problem [9].

As is well-known, (2.1) is usually put into a mixed form: find u and p such that

$$\mathbf{curl}\,\mathrm{curl}\,u + \nabla p = f, \quad \mathrm{div}\,u = g \quad \text{in } \Omega, \quad u \cdot \tau = 0, \quad p = 0 \quad \text{on } \Gamma. \tag{2.3}$$

If the solution pair (u, p) is smooth, we obtain by taking divergence on the first equation that

$$\Delta p = 0 \quad \text{in } \Omega, \quad p = 0 \quad \text{on } \Gamma, \tag{2.4}$$

since, from (2.1), f should satisfy the compatibility condition $\mathrm{div}\,f = 0$ in Ω. Then it can be easily seen that p is identically equal to zero on $\overline{\Omega}$. The role that p plays is the Lagrange multiplier, accounting for the divergence equation $\mathrm{div}\,u = g$. This multiplier is sometimes named as a dummy variable by engineers. For problem (2.3), a popular FEM is to use an $H(\mathrm{curl}; \Omega)$-conforming edge elements for u and an $H^1(\Omega)$-conforming elements for p. The mixed variational problem reads: find $u \in H_0(\mathrm{curl}; \Omega)$ and $p \in H_0^1(\Omega)$ such that

$$\begin{aligned}(\mathrm{curl}\,u, \mathrm{curl}\,v) + (\nabla p, v) &= (f, v) \quad \forall\, v \in H_0(\mathrm{curl}; \Omega), \\ (u, \nabla q) &= -(g, q) \quad \forall\, q \in H_0^1(\Omega),\end{aligned} \tag{2.5}$$

where the function spaces are defined as follows:

$$\begin{aligned}H^1(\Omega) &= \{q : q \in L^2(\Omega),\ \nabla q \in (L^2(\Omega))^2\}, \\ H_0^1(\Omega) &= \{q : q \in H^1(\Omega),\ q|_\Gamma = 0\}\end{aligned}$$

both with the standard inner product and associated norm, and

$$H(\mathrm{curl};\Omega) = \{v : \ v \in (L^2(\Omega))^2, \ \mathrm{curl}\,v \in L^2(\Omega)\},$$
$$H_0(\mathrm{curl};\Omega) = \{v : \ v \in H(\mathrm{curl};\Omega), \ v \cdot \tau|_\Gamma = 0\}$$

both with the following inner product and associated norm: for all $v, w \in H(\mathrm{curl};\Omega)$,

$$(v, w)_{H(\mathrm{curl})} := (v, w) + (\mathrm{curl}\,v, \mathrm{curl}\,w), \quad \|v\|_{H(\mathrm{curl})} := \left(\|v\|_0^2 + \|\mathrm{curl}\,v\|_0^2\right)^{1/2}.$$

From [27] (see Theorem 3.4 on page 243) we know that the solution u of (2.1) can be split into two parts: a regular part and a singular part, i.e., $u = u^R + \nabla p^S$, with $u^R \in (H^{1+r}(\Omega))^2$ and $p^S \in H^{1+r}(\Omega)$ for any $r < r_\Omega$. Here $r_\Omega > 1/2$ depends on Ω. Such split indicates that $u \in (H^r(\Omega))^2$ and $\mathrm{curl}\,u \in H^r(\Omega)$. For cracked polygonal domain (although not being Lipschitzian), the same results hold for $r_\Omega = 1/2$.

3. A mixed H^1-conforming finite element method. In this section, we shall introduce a mixed H^1-conforming FEM for solving (2.5). That is to say, we want to use the H^1-conforming elements for u as well, instead of the $H(\mathrm{curl};\Omega)$-conforming edge elements. It is seemingly not difficult to do so, but, as we have mentioned in the introduction section, the fact is that a simply direct application of H^1-conforming FEM would lead to a wrong convergence. This may happen if the exact solution u does not belong to H^1. The wrong convergence means that the H^1-conforming finite element solution (if it exists) from (2.5) would converge to an H^1 element, not to the true solution which is outside H^1 [10, 28, 32]. Another important fact is that the direct H^1-conforming FEM may not be stable, because the bilinear form $(\mathrm{curl}\,u, \mathrm{curl}\,v)$ may lack stability in the kernel set of $(v, \nabla q)$ in the H^1-conforming finite element space. In terms of the $\mathcal{K}_h$-coercivity (see Section 4) and the Babuška-Brezzi inf-sup condition, the $\mathcal{K}_h$-coercivity may fail. This fact is in sharp contrast to the continuous problem for which the bilinear form $(\mathrm{curl}\,u, \mathrm{curl}\,v)$ is coercive in the kernel set of $(v, \nabla q)$, e.g., see [3]. Consequently, problem (2.5) in H^1-conforming finite element spaces would even not possess a solution. Readers may refer to the classical book [17] for more details about the theory of saddle-point problems.

Let $\mathcal{T}_h$ be a conforming triangulation of Ω into shape-regular triangles [16, 20], where $h := \max_{T \in \mathcal{T}_h} h_T$ is the mesh parameter of the triangulation and h_T is the diameter of triangle T. On each T, we denote by $P_\ell(T)$ the space of polynomials of degree not greater than ℓ. Let $U_h \subset (H^1(\Omega))^2 \cap H_0(\mathrm{curl};\Omega)$ and $Q_h \subset H_0^1(\Omega)$ be the H^1-conforming finite element spaces for the unknowns u and p, respectively. The certain choices of U_h and Q_h will be specified in Section 5. To have a correct convergence and to have a stability, we propose the mixed H^1-conforming FEM which is formulated in the following stabilized form: find $u_h \in U_h \subset (H^1(\Omega))^2 \cap H_0(\mathrm{curl};\Omega)$ and $p_h \in Q_h \subset H_0^1(\Omega)$ such that for all $v_h \in U_h$ and $q_h \in Q_h$, we have

$$(\mathrm{curl}\,u_h, \mathrm{curl}\,v_h) + \sum_{T \in \mathcal{T}_h} h_T^2 (\mathrm{div}\,u_h, \mathrm{div}\,v_h)_{0,T} + (\nabla p_h, v_h) = (f, v_h) + \sum_{T \in \mathcal{T}_h} h_T^2 (g, \mathrm{div}\,v_h)_{0,T},$$
$$(u_h, \nabla q_h) = -(g, q_h), \tag{3.1}$$

where $(\cdot, \cdot)_{0,T}$ denotes the L^2 inner product over the element T. The mesh-dependent term plays the role of stabilization, a remedy to the lost stability from $(\mathrm{curl}\,u_h, \mathrm{curl}\,v_h)$ on the kernel set of $(v_h, \nabla q_h)$. Of course, for edge elements in $H(\mathrm{curl};\Omega)$ space, a coercivity indeed holds on this kernel set [1], without such stabilization. We note that (3.1) is still well-defined for edge elements. The stabilized mixed formulation (3.1) is therefore more interesting, since it can be used for both H^1-conforming elements and edge elements of $H(\mathrm{curl};\Omega)$-conforming only. The expression $(\nabla p_h, v_h)$ in (3.1) is exactly equal to $-(p_h, \mathrm{div}\,v_h)$, but the present analysis seems not to be improved with the use of the latter expression $-(p_h, \mathrm{div}\,v_h)$.

We now briefly summarize the differences of the proposed mixed H^1-conforming stabilized FEM (3.1) from the other methods in the literature:

- The method (3.1) is different from those in [18, 24, 28], where a global-defined over Ω weight function, denoted by w, which depends the geometrical singularities, is introduced to the divergence term:

$$(\operatorname{curl} \boldsymbol{u}_h, \operatorname{curl} \boldsymbol{v}_h) + (w \operatorname{div} \boldsymbol{u}_h, \operatorname{div} \boldsymbol{v}_h) + (\nabla p_h, \boldsymbol{v}_h) = (\boldsymbol{f}, \boldsymbol{v}_h) + (wg, \operatorname{div} \boldsymbol{v}_h),$$
$$(\boldsymbol{u}_h, \nabla q_h) = -(g, q_h). \tag{3.2}$$

- The method (3.1) is different from those in [32, 34, 35, 36, 37], where an L^2 inner product term of p_h is introduced:

$$(\operatorname{curl} \boldsymbol{u}_h, \operatorname{curl} \boldsymbol{v}_h) + \sum_{T \in \mathcal{T}_h} h_T^2 (\operatorname{div} \boldsymbol{u}_h, \operatorname{div} \boldsymbol{v}_h)_{0,T} + (\nabla p_h, \boldsymbol{v}_h) = (\boldsymbol{f}, \boldsymbol{v}_h) + \sum_{T \in \mathcal{T}_h} h_T^2 (g, \operatorname{div} \boldsymbol{v}_h)_{0,T},$$
$$(\boldsymbol{u}_h, \nabla q_h) - (p_h, q_h) = -(g, q_h). \tag{3.3}$$

- The method (3.1) is different from those in [7, 11, 14, 15], where mesh-dependent L^2 inner product terms with $\alpha \in (1/2, 1]$ are introduced:

$$(\operatorname{curl} \boldsymbol{u}_h, \operatorname{curl} \boldsymbol{v}_h) + h^{2\alpha} (\operatorname{div} \boldsymbol{u}_h, \operatorname{div} \boldsymbol{v}_h) + (\nabla p_h, \boldsymbol{v}_h) = (\boldsymbol{f}, \boldsymbol{v}_h) + h^{2\alpha} (g, \operatorname{div} \boldsymbol{v}_h),$$
$$(\boldsymbol{u}_h, \nabla q_h) - h^{2(1-\alpha)} (\nabla p_h, \nabla q_h) = -(g, q_h). \tag{3.4}$$

One can also see that the arguments which will be developed in this paper for the analysis of stability and error estimates are different from those in the above literature. Moreover, the H^1-conforming elements and their stability analysis and error estimates in our paper are new to Maxwell's equations. Finally, we should emphasize that the mixed H^1-conforming FEM (3.1) has not been studied so far, to the authors' knowledge.

4. A general framework of stability and error analysis. In this section, we provide a general framework of stability and error analysis for the mixed H^1-conforming FEM (3.1). We shall follow the classical theory for saddle-point problems as developed in the book of Brezzi and Fortin [17]. This consists of the verification of the $\mathcal{K}_h$-coercivity/stability and the Babuška-Brezzi inf-sup condition. We first introduce the bilinear forms $a(\cdot, \cdot) : (H_0(\operatorname{curl}; \Omega) \cap H(\operatorname{div}; \Omega)) \times (H_0(\operatorname{curl}; \Omega) \cap H(\operatorname{div}; \Omega)) \to \mathbb{R}$ and $b(\cdot, \cdot) : H_0(\operatorname{curl}; \Omega) \times H_0^1(\Omega) \to \mathbb{R}$ by

$$a(\boldsymbol{u}, \boldsymbol{v}) = (\operatorname{curl} \boldsymbol{u}, \operatorname{curl} \boldsymbol{v}) + \sum_{T \in \mathcal{T}_h} h_T^2 (\operatorname{div} \boldsymbol{u}, \operatorname{div} \boldsymbol{v})_{0,T}, \tag{4.1}$$

$$b(\boldsymbol{v}, q) = (\nabla q, \boldsymbol{v}), \tag{4.2}$$

and then define the kernel set $\mathcal{K}_h$ by

$$\mathcal{K}_h := \{\boldsymbol{v}_h \in U_h : \ b(\boldsymbol{v}_h, q_h) = 0, \ \forall \, q_h \in Q_h\}. \tag{4.3}$$

Define an H^1 finite element projection $R_h : \chi \in H^{-1}(\Omega) \to R_h(\chi) \in Q_h$ as follows:

$$(R_h(\chi), q_h)_1 := (\nabla R_h(\chi), \nabla q_h) = \langle \chi, q_h \rangle \quad \forall \, q_h \in Q_h, \tag{4.4}$$

where $\langle \cdot, \cdot \rangle$ denotes the duality pairing between $H^{-1}(\Omega)$ (the dual of $H_0^1(\Omega)$) and $H_0^1(\Omega)$. Such R_h is actually the discrete version of the so-called Riesz-representation operator, denoted by $R : H^{-1}(\Omega) \to H_0^1(\Omega)$, which is defined by $(R(\chi), q)_1 := \langle \chi, q \rangle$ for all $q \in H_0^1(\Omega)$. Now, for any $\boldsymbol{v} \in (L^2(\Omega))^2$, since $\operatorname{div} \boldsymbol{v} \in H^{-1}(\Omega)$, we have

$$(R_h(\operatorname{div} \boldsymbol{v}), q_h)_1 = \langle \operatorname{div} \boldsymbol{v}, q_h \rangle = -(\nabla q_h, \boldsymbol{v}) \quad \forall \, q_h \in Q_h. \tag{4.5}$$

It can be seen that for any $v \in (L^2(\Omega))^2$,

$$|R_h(\text{div}\, v)|_1 \leq \|v\|_0,$$

where $|\cdot|_1$ denotes the H^1 semi-norm, i.e., $|q|_1 = \sqrt{(q,q)_1} = \sqrt{(\nabla q, \nabla q)}$. Throughout this paper, we let C denote a generic positive constant, possibly different at different occurrences, which is always independent of the mesh parameter h.

PROPOSITION 4.1. *We have*

$$|||v_h|||_h^2 := \|\text{curl}\, v_h\|_0^2 + |R_h(\text{div}\, v_h)|_1^2 + \sum_{T \in \mathcal{T}_h} h_T^2 \|\text{div}\, v_h\|_{0,T}^2 \geq C\|v_h\|_0^2 \quad \forall\, v_h \in U_h. \tag{4.6}$$

Proof. We show (4.6) following the argument in [32] (see Theorem 4.1 on pages 1287-1290). Introducing two function spaces,

$$H(\text{div}; \Omega) = \{v \in (L^2(\Omega))^2 : \text{div}\, v \in L^2(\Omega)\},$$
$$H(\text{div}0; \Omega) = \{v \in H(\text{div}; \Omega) : \text{div}\, v = 0\},$$

we have by the L^2-orthogonal decomposition that

$$v_h = \boldsymbol{\phi} + \nabla q, \quad \boldsymbol{\phi} \in H(\text{curl}; \Omega) \cap H(\text{div}0; \Omega), \quad q \in H_0^1(\Omega),$$

$$\|v_h\|_0^2 = \|\boldsymbol{\phi}\|_0^2 + \|\nabla q\|_0^2.$$

Since $v_h \in H_0(\text{curl}; \Omega)$, we see that $\boldsymbol{\phi} \in H_0(\text{curl}; \Omega)$, and that there holds the Poincaré inequality on $H_0(\text{curl}; \Omega) \cap H(\text{div}0; \Omega)$,

$$\|\boldsymbol{\phi}\|_0 \leq C\|\text{curl}\, \boldsymbol{\phi}\|_0 = C\|\text{curl}\, v_h\|_0.$$

We then find that

$$\|v_h\|_0^2 \leq C\big(\|\text{curl}\, v_h\|_0^2 + |q|_1^2\big).$$

Let $q_h \in Q_h \subset H_0^1(\Omega)$ denote a finite element interpolation of $q \in H_0^1(\Omega)$, satisfying

$$\left(\sum_{T \in \mathcal{T}_h} h_T^{-2} \|q_h - q\|_{0,T}^2\right)^{1/2} + \|q_h\|_1 \leq C\|q\|_1,$$

where $\|q\|_1^2 = \|q\|_0^2 + |q|_1^2$, satisfying $\|q\|_1 \leq C|q|_1$. Taking a constant $\alpha > 0$ to be determined, we have

$$|R_h(\text{div}\, v_h)|_1^2 = |R_h(\text{div}\, v_h) + \alpha q_h|_1^2 - 2\alpha\big(R_h(\text{div}\, v_h), q_h\big)_1 - \alpha^2|q_h|_1^2.$$

Below we estimate the last two terms in the above. Firstly,

$$|q_h|_1^2 \leq C|q|_1^2.$$

Secondly,

$$-2\alpha\big(R_h(\text{div}\, v_h), q_h\big)_1 = 2\alpha(v_h, \nabla q_h) = 2\alpha\big(v_h, \nabla(q_h - q)\big) + 2\alpha(v_h, \nabla q),$$

where

$$2\alpha(\boldsymbol{v}_h, \nabla q) = 2\alpha(\boldsymbol{\phi} + \nabla q, \nabla q) = 2\alpha\|\nabla q\|_0^2 = 2\alpha|q|_1^2$$

and

$$2\alpha\big(\boldsymbol{v}_h, \nabla(q_h - q)\big) = -2\alpha(\operatorname{div}\boldsymbol{v}_h, q_h - q)$$
$$\geq -2\alpha\Big(\sum_{T\in\mathcal{T}_h} h_T^2\|\operatorname{div}\boldsymbol{v}_h\|_{0,T}^2\Big)^{1/2}\Big(\sum_{T\in\mathcal{T}_h} h_T^{-2}\|q_h - q\|_{0,T}^2\Big)^{1/2}$$
$$\geq -2\alpha C\|q\|_1\Big(\sum_{T\in\mathcal{T}_h} h_T^2\|\operatorname{div}\boldsymbol{v}_h\|_{0,T}^2\Big)^{1/2} \geq -2\alpha C|q|_1\Big(\sum_{T\in\mathcal{T}_h} h_T^2\|\operatorname{div}\boldsymbol{v}_h\|_{0,T}^2\Big)^{1/2}$$
$$\geq -\sum_{T\in\mathcal{T}_h} h_T^2\|\operatorname{div}\boldsymbol{v}_h\|_{0,T}^2 - \alpha^2 C|q|_1^2.$$

Thus, putting $0 < \alpha := 1/(2C)$, we have

$$|R_h(\operatorname{div}\boldsymbol{v}_h)|_1^2 = |R_h(\operatorname{div}\boldsymbol{v}_h) + \alpha q_h|_1^2 - 2\alpha\big(R_h(\operatorname{div}\boldsymbol{v}_h), q_h\big)_1 - \alpha^2|q_h|_1^2$$
$$\geq |R_h(\operatorname{div}\boldsymbol{v}_h) + \alpha q_h|_1^2 + \alpha(2 - 2\alpha C)|q|_1^2 - \sum_{T\in\mathcal{T}_h} h_T^2\|\operatorname{div}\boldsymbol{v}_h\|_{0,T}^2$$
$$\geq \alpha|q|_1^2 - \sum_{T\in\mathcal{T}_h} h_T^2\|\operatorname{div}\boldsymbol{v}_h\|_{0,T}^2.$$

That is,

$$\alpha|q|_1^2 \leq |R_h(\operatorname{div}\boldsymbol{v}_h)|_1^2 + \sum_{T\in\mathcal{T}_h} h_T^2\|\operatorname{div}\boldsymbol{v}_h\|_{0,T}^2.$$

Finally, we have

$$\|\boldsymbol{v}_h\|_0^2 \leq C\big(\|\operatorname{curl}\boldsymbol{v}_h\|_0^2 + |q|_1^2\big) \leq C\max\{1, 1/\alpha\}\big(\|\operatorname{curl}\boldsymbol{v}_h\|_0^2 + \alpha|q|_1^2\big)$$
$$\leq C\max\{1, 1/\alpha\}\Big(\|\operatorname{curl}\boldsymbol{v}_h\|_0^2 + |R_h(\operatorname{div}\boldsymbol{v}_h)|_1^2 + \sum_{T\in\mathcal{T}_h} h_T^2\|\operatorname{div}\boldsymbol{v}_h\|_{0,T}^2\Big),$$

which is the desired (4.6). This completes the proof. $\square$

LEMMA 4.2. *The following $\mathcal{K}_h$-coercvity/stability holds:*

$$a(\boldsymbol{v}_h, \boldsymbol{v}_h) \geq C\|\boldsymbol{v}_h\|_0^2 \quad \forall\, \boldsymbol{v}_h \in \mathcal{K}_h. \tag{4.7}$$

Proof. For any given $\boldsymbol{v}_h \in U_h$, from Proposition 4.1, we have

$$|||\boldsymbol{v}_h|||_h^2 = \|\operatorname{curl}\boldsymbol{v}_h\|_0^2 + |R_h(\operatorname{div}\boldsymbol{v}_h)|_1^2 + \sum_{T\in\mathcal{T}_h} h_T^2\|\operatorname{div}\boldsymbol{v}_h\|_{0,T}^2 \geq C\|\boldsymbol{v}_h\|_0^2 \quad \forall\, \boldsymbol{v}_h \in U_h.$$

But, noticing that

$$\mathcal{K}_h = \{\boldsymbol{v}_h \in U_h :\ b(\boldsymbol{v}_h, q_h) = 0,\ \forall\, q_h \in Q_h\} = \{\boldsymbol{v}_h \in U_h : R_h(\operatorname{div}\boldsymbol{v}_h) = 0\}, \tag{4.8}$$

and that

$$a(\boldsymbol{v}_h, \boldsymbol{v}_h) = \|\operatorname{curl}\boldsymbol{v}_h\|_0^2 + \sum_{T\in\mathcal{T}_h} h_T^2\|\operatorname{div}\boldsymbol{v}_h\|_{0,T}^2,$$

we immediately conclude that (4.7) holds. $\square$

THEOREM 4.3. *Assume that (U_h, Q_h) satisfies the following Babuška-Brezzi inf-sup condition:*

$$\sup_{\boldsymbol{v}_h \in U_h} \frac{b(\boldsymbol{v}_h, q_h)}{|||\boldsymbol{v}_h|||_h} \geq C \|q_h\|_0 \quad \forall \, q_h \in Q_h. \tag{4.9}$$

Then, for any $\boldsymbol{f} \in H(\mathrm{div}0; \Omega)$ and $g \in L^2(\Omega)$, problem (3.1) admits a unique solution $(\boldsymbol{u}_h, p_h) \in U_h \times Q_h$.

Proof. Firstly, for all $\boldsymbol{v}_h \in \mathcal{K}_h$, we have from (4.8) $R_h(\mathrm{div}\, \boldsymbol{v}_h) = 0$, and from (4.6) we see that

$$a(\boldsymbol{v}_h, \boldsymbol{v}_h) = |||\boldsymbol{v}_h|||_h^2. \tag{4.10}$$

With (4.9) at hand, the conclusion is just a simple consequence of the classical theory in [17]. $\square$

From the classical theory [17], consequently, we have the following error estimates:

THEOREM 4.4. *Assume that the inf-sup condition (4.9) holds. Let $(\boldsymbol{u}, p)$ denote the exact solution of Maxwell's equations (2.3) and $(\boldsymbol{u}_h, p_h)$ the finite element solution of (3.1) in $U_h \times Q_h$. Then for all $(\boldsymbol{v}_h, q_h) \in U_h \times Q_h$, we have*

$$|||\boldsymbol{u} - \boldsymbol{u}_h|||_h + \|p - p_h\|_0 \leq C\left(|||\boldsymbol{u} - \boldsymbol{v}_h|||_h + \|p - q_h\|_1\right) + C \sup_{\mu_h \in Q_h} \frac{(\nabla \mu_h, \boldsymbol{u} - \boldsymbol{v}_h)}{\|\mu_h\|_0}. \tag{4.11}$$

Proof. Adapting the arguments in [17] for proving both Proposition 2.4 on page 54, Proposition 2.5 on page 55, and Proposition 2.7 on page 56, we can show (4.11). For the sake of completeness, we prove (4.11) in details. For this purpose, we introduce the set

$$\mathcal{K}_h(g) := \{\boldsymbol{v}_h \in U_h : \ (\boldsymbol{v}_h, \nabla q_h) = -(g, q_h), \forall \, q_h \in Q_h\}. \tag{4.12}$$

For $g = 0$, $\mathcal{K}_h(0) = \mathcal{K}_h$ which is defined by (4.3). Moreover, for any $g \in L^2(\Omega)$, as has been shown by Theorem 4.3,

$$\mathcal{K}_h(g) \neq \varnothing. \tag{4.13}$$

Firstly, we show that

$$|||\boldsymbol{u} - \boldsymbol{u}_h|||_h \leq C \left(\inf_{\boldsymbol{w}_h \in \mathcal{K}_h(g)} |||\boldsymbol{u} - \boldsymbol{w}_h|||_h + \inf_{q_h \in Q_h} \|p - q_h\|_1 \right). \tag{4.14}$$

We step-by-step follow the argument in proving Proposition 2.4 on page 54 in [17]. In fact, let $\boldsymbol{w}_h$ be any element of $\mathcal{K}_h(g)$. Since $\boldsymbol{w}_h - \boldsymbol{u}_h \in \mathcal{K}_h$, from (4.10) we have

$$C|||\boldsymbol{w}_h - \boldsymbol{u}_h|||_h \leq \sup_{\boldsymbol{z}_h \in \mathcal{K}_h} \frac{a(\boldsymbol{w}_h - \boldsymbol{u}_h, \boldsymbol{z}_h)}{|||\boldsymbol{z}_h|||_h}, \tag{4.15}$$

where

$$a(\boldsymbol{w}_h - \boldsymbol{u}_h, \boldsymbol{z}_h) = a(\boldsymbol{w}_h - \boldsymbol{u}, \boldsymbol{z}_h) + a(\boldsymbol{u} - \boldsymbol{u}_h, \boldsymbol{z}_h),$$

but, for $(\boldsymbol{u}, p)$ the exact solution and $(\boldsymbol{u}_h, p_h)$ the finite element solution, from (2.1), (2.5) and (3.1), we find that

$$a(\boldsymbol{u} - \boldsymbol{u}_h, \boldsymbol{z}_h) = -b(\boldsymbol{z}_h, p - p_h).$$

As $z_h \in \mathcal{K}_h$, for any $q_h \in Q_h$, from Lemma 4.2, we have

$$|b(z_h, p - p_h)| = |b(z_h, p - q_h)| \leq ||z_h||_0 ||\nabla(p - q_h)||_0 \leq C|||z_h|||_h ||p - q_h||_1,$$

and (4.15) becomes

$$
\begin{aligned}
C|||\boldsymbol{w}_h - \boldsymbol{u}_h|||_h &\leq \sup_{\boldsymbol{z}_h \in \mathcal{K}_h} \frac{a(\boldsymbol{w}_h - \boldsymbol{u}_h, \boldsymbol{z}_h)}{|||\boldsymbol{z}_h|||_h} = \sup_{\boldsymbol{z}_h \in \mathcal{K}_h} \frac{a(\boldsymbol{w}_h - \boldsymbol{u}, \boldsymbol{z}_h) - b(\boldsymbol{z}_h, p - q_h)}{|||\boldsymbol{z}_h|||_h} \\
&\leq C(|||\boldsymbol{u} - \boldsymbol{w}_h|||_h + ||p - q_h||_1),
\end{aligned}
\tag{4.16}
$$

and (4.14) follows using the triangle inequality.

Secondly, we use the inf-sup condition (4.9) to show that

$$\inf_{\boldsymbol{w}_h \in \mathcal{K}_h(g)} |||\boldsymbol{u} - \boldsymbol{w}_h|||_h \leq C \inf_{\boldsymbol{v}_h \in U_h} \left(|||\boldsymbol{u} - \boldsymbol{v}_h|||_h + \sup_{\mu_h \in Q_h} \frac{(\nabla \mu_h, \boldsymbol{u} - \boldsymbol{v}_h)}{||\mu_h||_0} \right). \tag{4.17}$$

We show (4.17) step-by-step reproducing the argument in proving Proposition 2.5 on page 55 in [17]. Note that from the inf-sup condition (4.9), similar to (1.15) and (1.16) on page 39 in [17] which result from Proposition 1.2 on the same page, for any $\boldsymbol{t}_h \in U_h/\mathcal{K}_h$, we have

$$C|||\boldsymbol{t}_h|||_h \leq \sup_{\mu_h \in Q_h} \frac{b(\boldsymbol{t}_h, \mu_h)}{||\mu_h||_0}. \tag{4.18}$$

With (4.18) at hand, we can exactly reproduce the argument in proving Proposition 2.5 on page 55 in [17] to obtain (4.17). Let $\boldsymbol{v}_h$ be any element of U_h. We look for $\boldsymbol{r}_h \in U_h$ such that

$$b(\boldsymbol{r}_h, \mu_h) = b(\boldsymbol{u} - \boldsymbol{v}_h, \mu_h) \quad \forall \mu_h \in Q_h. \tag{4.19}$$

With $g' := g + \operatorname{div} \boldsymbol{v}_h$, (4.13) ensures that (4.19) has at least one solution. From Proposition 1.2 on page 39 in [17] and (4.18), we can in fact find a solution satisfying

$$|||\boldsymbol{r}_h|||_h \leq C \sup_{\mu_h \in Q_h} \frac{(\nabla \mu_h, \boldsymbol{u} - \boldsymbol{v}_h)}{||\mu_h||_0}. \tag{4.20}$$

From (4.19), we also know that $\boldsymbol{w}_h := \boldsymbol{r}_h + \boldsymbol{v}_h \in \mathcal{K}_h(g)$. Thus, writing

$$|||\boldsymbol{u} - \boldsymbol{w}_h|||_h = |||\boldsymbol{u} - \boldsymbol{v}_h - \boldsymbol{r}_h|||_h \leq |||\boldsymbol{u} - \boldsymbol{v}_h|||_h + |||\boldsymbol{r}_h|||_h,$$

we get directly (4.17) from (4.20).

Thirdly, trivially and exactly, step-by-step reproducing the argument in proving Proposition 2.7 on page 56 in [17], from the inf-sup condition (4.9), we obtain the estimate for $p - p_h$:

$$||p - p_h||_0 \leq C \left(\inf_{q_h \in Q_h} ||p - q_h||_1 + |||\boldsymbol{u} - \boldsymbol{u}_h|||_h \right). \tag{4.21}$$

Hence, from (4.14), (4.17) and (4.21), it follows that (4.11) holds. This completes the proof. □

Note that the term $||p - q_h||_1$ in the right-hand side of (4.11) cannot be replaced by $||p - q_h||_0$, because the divergence norm $||\operatorname{div} \cdot ||_0$ of $\boldsymbol{v}_h$ does not appear in the norm $|||\boldsymbol{v}_h|||_h$, while the mesh-dependent divergence norm $(\sum_{T \in \mathcal{T}_h} h_T^2 ||\operatorname{div} \cdot ||_{0,T}^2)^{1/2}$ in $||| \cdot |||_h$ is too weak.
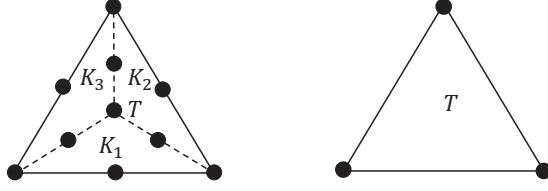
FIG. 5.1. *(left) P_2 elements for u_h with the Clough-Tocher refinement, $T = \cup_{i=1}^{3} K_i$; (right) P_1 elements for p_h.*

5. Error estimates of CP_2-P_1 elements. In this section, we first consider the H^1-conforming composite quadratic elements for u_h and the standard P_1 elements for p_h and then establish the error bound between the exact solution (u, p) of (2.3) and the finite element solution (u_h, p_h) of (3.1). Define a sub-mesh $\mathcal{T}_{h/2}$ from the original triangulation $\mathcal{T}_h$, by connecting the three vertices of each triangle element to the interior barycentric point. This is the so-called Clough-Tocher refinement [51], see Figure 5.1. Thus, each $T \in \mathcal{T}_h$ is the union of three sub-triangle elements in $\mathcal{T}_{h/2}$. We introduce the finite element spaces,

$$U_h = \{v_h \in (H^1(\Omega))^2 \cap H_0(\text{curl}; \Omega) : \; v_h|_{K_i} \in (P_2(K_i))^2, i = 1, 2, 3, \; \forall \, T \in \mathcal{T}_h, \; T = \cup_{i=1}^{3} K_i\}, \qquad (5.1)$$

$$Q_h = \{q_h \in H_0^1(\Omega) : \; q_h|_T \in P_1(T), \forall \, T \in \mathcal{T}_h\}. \qquad (5.2)$$

The pair (U_h, Q_h) will be called the CP_2-P_1 elements in this paper. This finite element pair CP_2-P_1 is stable, i.e., the inf-sup condition (4.9) in Theorem 4.3 holds, see Theorem 5.2 below for the verification.

To establish the error bound, we recall that the solution u of (2.1) admits a so-called regular-singular decomposition:

$$u = u^R + \nabla p^S, \qquad (5.3)$$

where u^R is the regular part, belonging to $(H^{1+r}(\Omega))^2 \cap H_0(\text{curl}; \Omega)$, and ∇p^S is the singular part with $p^S \in H^{1+r}(\Omega) \cap H_0^1(\Omega)$, for some $0 \leq r \leq 1$. In [27, 30], it is shown that the above decomposition holds in the case of $g = 0$. Therefore, it can be expected that if $g \neq 0$ and $g \in L^2(\Omega)$, the same decomposition would hold. In fact, we can lift the equation $\text{div} \, u = g$ by a particular solution $u_0 = \nabla \varphi$ where $\varphi \in H_0^1(\Omega)$ solves $\Delta \varphi = g$ in Ω. Then, consider $u - u_0$ that satisfies $\text{div} \, (u - u_0) = 0$ and $\text{curl curl} \, (u - u_0) = \text{curl curl} \, u$. Since $\varphi \in H^{1+r}(\Omega)$ by the regularity result for the Dirichlet Laplacian, from the regular-singular decomposition in the form of (5.3) of $u - u_0$, we still obtain a regular-singular decomposition in the form of (5.3) for u. Readers may also refer to [23].

Let W_h denote the Hsieh-Clough-Tocher C^1 finite element space of $H_0^1(\Omega) \cap H^2(\Omega)$. As is pointed out in [28], U_h contains the gradient of the Hsieh-Clough-Tocher C^1 elements which are of piecewise P_3 polynomials, i.e., $\nabla W_h \subset U_h$. Readers may refer to [4, 5, 20, 21, 47, 48, 49, 50, 51, 52, 53] for details of C^1 elements. Since on each triangle element, W_h consists of piecewise P_3 polynomials, it could be shown that there exists $A_h p^S \in W_h$, the finite element interpolation of p^S, satisfying

$$\|A_h p^S - p^S\|_0 + h|A_h p^S - p^S|_1 \leq Ch^{1+r}\|p^S\|_{1+r}, \qquad (5.4)$$

$$\int_F (A_h p^S - p^S) = 0 \quad \forall \, F \subset \partial T, \; \forall \, T \in \mathcal{T}_h. \qquad (5.5)$$

We remark that both (5.4) and (5.5) can also be satisfied by some C^0 elements. For example, the C^0 quadratic element can satisfy (5.4) and (5.5), see Lemma A.3 on page 100 of [43]. More than (5.4) and (5.5), $\nabla A_h p^S \in U_h \subset (H^1(\Omega))^2$. It can be seen that both (5.5) and the fact that Q_h contains P_1 element only imply

$$\left(\nabla q_h, \nabla(A_h p^S - p^S)\right) = \sum_{T \in \mathcal{T}_h} \int_{\partial T} \nabla q_h \cdot \mathbf{n}(A_h p^S - p^S) = 0 \quad \forall\, q_h \in Q_h. \tag{5.6}$$

Further, from (4.5) and (5.6), we find that

$$\left(R_h(\mathrm{div}\,(\nabla(p^S - A_h p^S))), q_h\right)_1 = -\left(\nabla q_h, \nabla(p^S - A_h p^S)\right) = 0. \tag{5.7}$$

Let $\Pi_h \mathbf{u}^R \in U_h$ denote any classical H^1-conforming finite element interpolation [20, 21]. Then we have

$$\|\Pi_h \mathbf{u}^R - \mathbf{u}^R\|_0 + h|\Pi_h \mathbf{u}^R - \mathbf{u}^R|_1 \le Ch^{1+r}\|\mathbf{u}^R\|_{1+r}. \tag{5.8}$$

Since

$$\nabla A_h p^S \in U_h, \tag{5.9}$$

we denote by

$$\tilde{\mathbf{u}}_h := \Pi_h \mathbf{u}^R + \nabla A_h p^S \in U_h \tag{5.10}$$

the finite element interpolation of $\mathbf{u}$. With this $\tilde{\mathbf{u}}_h$, we first have

$$\|\mathbf{u} - \tilde{\mathbf{u}}_h\|_0 \le Ch^r \left(\|\mathbf{u}^R\|_{1+r} + \|p^S\|_{1+r}\right), \tag{5.11}$$

$$\|\mathrm{curl}\,(\mathbf{u} - \tilde{\mathbf{u}}_h)\|_0 = \|\mathrm{curl}\,(\mathbf{u}^R - \Pi_h \mathbf{u}^R)\|_0 \le C|\mathbf{u}^R - \Pi_h \mathbf{u}^R|_1 \le Ch^r\|\mathbf{u}^R\|_{1+r}. \tag{5.12}$$

Moreover, from (4.5), (5.6) and (5.8), we have

$$\begin{aligned}
|R_h(\mathrm{div}\,(\mathbf{u} - \tilde{\mathbf{u}}_h))|_1^2 &= -\left(\nabla R_h(\mathrm{div}\,(\mathbf{u} - \tilde{\mathbf{u}}_h)), \mathbf{u} - \tilde{\mathbf{u}}_h\right) \\
&= -\left(\nabla R_h(\mathrm{div}\,(\mathbf{u} - \tilde{\mathbf{u}}_h)), \mathbf{u}^R - \Pi_h \mathbf{u}\right) \\
&\le Ch^{1+r}\|\mathbf{u}^R\|_{1+r}|R_h(\mathrm{div}\,(\mathbf{u} - \tilde{\mathbf{u}}_h))|_1,
\end{aligned} \tag{5.13}$$

that is,

$$|R_h(\mathrm{div}\,(\mathbf{u} - \tilde{\mathbf{u}}_h))|_1 \le Ch^{1+r}\|\mathbf{u}^R\|_{1+r}. \tag{5.14}$$

Hence, we have

$$\|\mathrm{curl}\,(\mathbf{u} - \tilde{\mathbf{u}}_h)\|_0 + |R_h(\mathrm{div}\,(\mathbf{u} - \tilde{\mathbf{u}}_h))|_1 \le Ch^r\|\mathbf{u}^R\|_{1+r}. \tag{5.15}$$

To estimate the term

$$\left(\sum_{T \in \mathcal{T}_h} h_T^2 \|\mathrm{div}\,(\mathbf{u} - \tilde{\mathbf{u}}_h)\|_{0,T}^2\right)^{1/2}, \tag{5.16}$$

we can follow the same argument in [36] to establish the following result (see Proposition A.1 in the Appendix of this paper):

$$\left(\sum_{T \in \mathcal{T}_h} h_T^2 \|\mathrm{div}\,(\mathbf{u} - \tilde{\mathbf{u}}_h)\|_{0,T}^2\right)^{1/2} \le Ch^r \left(\|\mathbf{u}^R\|_{1+r} + \|p^S\|_{1+r} + \|\mathrm{div}\,\mathbf{u}\|_0\right). \tag{5.17}$$

Combining (5.15) and (5.17), we have

$$|||\boldsymbol{u} - \tilde{\boldsymbol{u}}_h|||_h \le Ch^r \big(\|\boldsymbol{u}^R\|_{1+r} + \|p^S\|_{1+r} + \|\operatorname{div}\boldsymbol{u}\|_0 \big). \tag{5.18}$$

Furthermore, following the same argument in proving (5.7) and (5.13), with $v_h := \tilde{\boldsymbol{u}}_h$, we find that

$$\sup_{\mu_h \in Q_h} \frac{(\nabla \mu_h, \boldsymbol{u} - \tilde{\boldsymbol{u}}_h)}{\|\mu_h\|_0} \le Ch^r \big(\|\boldsymbol{u}^R\|_{1+r} + \|p^S\|_{1+r} \big). \tag{5.19}$$

In addition, let $I_h p \in Q_h$ denote any classical H^1-conforming finite element interpolation of p, satisfying

$$\|I_h p - p\|_0 + h|I_h p - p|_1 \le Ch^r\|p\|_{1+r}. \tag{5.20}$$

However, since $p = 0$ in our case, then we just take $I_h p = 0$, i.e.,

$$\|p - I_h p\|_1 = 0. \tag{5.21}$$

From Theorem 4.4, therefore, we obtain the following error bound:

THEOREM 5.1. *Let* $(\boldsymbol{u}, p = 0)$ *denote the exact solution of Maxwell's equations (2.3) and* $(\boldsymbol{u}_h, p_h)$ *the solution of problem (3.1) using* CP_2-P_1 *elements. Assume that the regular-singular decomposition (5.3) holds. Then we have*

$$|||\boldsymbol{u} - \boldsymbol{u}_h|||_h + \|p - p_h\|_0 \le Ch^r \big(\|\boldsymbol{u}^R\|_{1+r} + \|p^S\|_{1+r} + \|\operatorname{div}\boldsymbol{u}\|_0 \big). \tag{5.22}$$

Note that by the triangle inequality, (5.11), (4.6), (5.22) and (5.18), we can further obtain

$$\|\boldsymbol{u} - \boldsymbol{u}_h\|_0 \le C(\|\boldsymbol{u} - \tilde{\boldsymbol{u}}\|_0 + \|\tilde{\boldsymbol{u}} - \boldsymbol{u}_h\|_0) \le Ch^r \big(\|\boldsymbol{u}^R\|_{1+r} + \|p^S\|_{1+r} + \|\operatorname{div}\boldsymbol{u}\|_0 \big). \tag{5.23}$$

In what follows, we turn to verify the fact that the CP_2-P_1 elements satisfy the Babuška-Brezzi inf-sup condition (4.9) as stated in Theorem 4.3. For that goal, we consider the following problem: for any given $q_h \in Q_h$, find $\theta \in H_0^1(\Omega)$ such that

$$-\Delta\theta = q_h \quad \text{in } \Omega, \quad \theta = 0 \quad \text{on } \partial\Omega.$$

It is known that

$$\theta \in H^{1+r}(\Omega), \quad \boldsymbol{v}^* = \nabla\theta \in (H^r(\Omega))^2, \quad r \ge 0,$$
$$-\operatorname{div}\boldsymbol{v}^* = q_h,$$
$$\|\boldsymbol{v}^*\|_s + \|\operatorname{div}\boldsymbol{v}^*\|_0 \le C\|q_h\|_0 \quad 0 \le s \le r.$$

Note that $r > \frac{1}{2}$ for Lipschitz polygons. Put $\boldsymbol{v}_h^* = \nabla(A_h\theta)$. Both (5.6) and (5.7) lead to

$$(\boldsymbol{v}^* - \boldsymbol{v}_h^*, \nabla q_h) = 0 \quad \forall\, q_h \in Q_h,$$

that is,

$$b(\boldsymbol{v}_h^* - \boldsymbol{v}^*, q_h) = 0 \quad \forall\, q_h \in Q_h.$$

Thus,

$$b(\boldsymbol{v}_h^*, q_h) = b(\boldsymbol{v}_h^* - \boldsymbol{v}^*, q_h) + b(\boldsymbol{v}^*, q_h) = b(\boldsymbol{v}^*, q_h) = (\boldsymbol{v}^*, \nabla q_h) = -(\operatorname{div}\boldsymbol{v}^*, q_h) = \|q_h\|_0^2,$$

$$|||\boldsymbol{v}_h^*|||_h = \Big(\sum_{T \in \mathcal{T}_h} h_T^2 \|\operatorname{div}\boldsymbol{v}_h^*\|_{0,T}^2 \Big)^{\frac{1}{2}} + |R_h(\operatorname{div}\boldsymbol{v}_h^*)|_1 \le C\|\boldsymbol{v}_h^*\|_0 \le C\|\theta\|_1 \le C\|q_h\|_0,$$
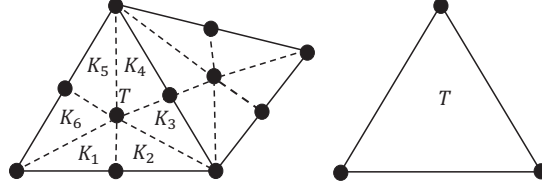
FIG. 5.2. *(left) P_1 elements for $\boldsymbol{u}_h$ with the Powell-Sabin refinement, $T = \cup_{i=1}^6 K_i$; (right) P_1 elements for p_h.*

where we have used the element local inverse estimates in [20, 21], $|v_h^*|_{1,T} \leq Ch_T^{-1}\|v_h^*\|_{0,T}$ for all $T \in \mathcal{T}_h$, and the boundedness of the H^1-projection R_h, i.e., $|R_h(\operatorname{div} v_h^*)|_1 \leq \|v_h^*\|_0$. Combining these we obtain

$$\sup_{\boldsymbol{v}_h \in U_h} \frac{b(\boldsymbol{v}_h, q_h)}{|||\boldsymbol{v}_h|||_h} \geq \frac{b(\boldsymbol{v}_h^*, q_h)}{|||\boldsymbol{v}_h^*|||_h} \geq C\|q_h\|_0.$$

The conclusion is stated as follows:

THEOREM 5.2. *For CP_2-P_1 elements, we have the Babuška-Brezzi inf-sup condition,*

$$\sup_{\boldsymbol{v}_h \in U_h} \frac{b(\boldsymbol{v}_h, q_h)}{|||\boldsymbol{v}_h|||_h} \geq C\|q_h\|_0 \quad \forall\, q_h \in Q_h. \tag{5.24}$$

We conclude this section with remarks on the finite elements CP_1-P_1 and P_2-P_1, and Maxwell's eigenvalue problems.

REMARK 5.3. *Theorem 5.1 and Theorem 5.2 are still valid for similar finite element spaces such as the CP_1-P_1 elements with the Powell-Sabin refinement [51] of the original triangulation. The related C^1 elements on the Powell-Sabin meshes are piecewise P_2 polynomials; see [47, 48, 49, 50, 51, 52, 53] for more C^1 elements on composite meshes. Let $\mathcal{T}_h$ be a triangulation, and suppose that for each triangle T, c denotes its incenter. For each triangle T, connect c to each of the three vertices of T. Connect c and c' by a straight line whenever the triangles T and T' share a common edge. In addition, connect the middle of each boundary edge to the incenter of the associated triangle, see Figure 5.2. Now, define the CP_1-P_1 finite element spaces U_h and Q_h by*

$$U_h = \{\boldsymbol{v}_h \in H_0(\mathrm{curl};\Omega) \cap (H^1(\Omega))^2 : \boldsymbol{v}_h|_{K_i} \in (P_1(K_i))^2,\ i = 1,2,\cdots,6, \forall\, T \in \mathcal{T}_h,\ T = \cup_{i=1}^6 K_i\},$$
$$Q_h = \{q_h \in H_0^1(\Omega) : q_h|_T \in P_1(T), \forall\, T \in \mathcal{T}_h\}.$$

REMARK 5.4. *In Section 6, we have performed numerical experiments for the P_2-P_1 elements, which are well-known as Taylor-Hood elements [8, 17, 43] in computational fluid dynamics. Since (3.1) is close to the Stokes equations, it would be interesting to use these elements. For P_2-P_1 elements, however, it seems that the argument for establishing Theorem 5.1 and Theorem 5.2 could not longer be valid, and both theorems seem not to be true. Nevertheless, numerical results reported in Section 6 support that such P_2-P_1 elements can be used for seeking the finite element solution of a non-H^1 very weak solution, with the desired convergence order r.*

REMARK 5.5. *The proposed mixed H^1-conforming FEM (3.1) can be straightforwardly applied to Maxwell's eigenvalue problems. Although we have not analyzed the eigenvalue problem, the numerical results reported in Section 6 show that the present method can indeed work for solving the eigenvalue problem. We will see that the computed convergence rate of the eigenvalue is about the twice of that of the regularity of the corresponding non-H^1 eigenfunction, i.e., if the error bound for the source problem is $O(h^r)$, then the error bound for eigenvalues is $O(h^{2r})$, as is*
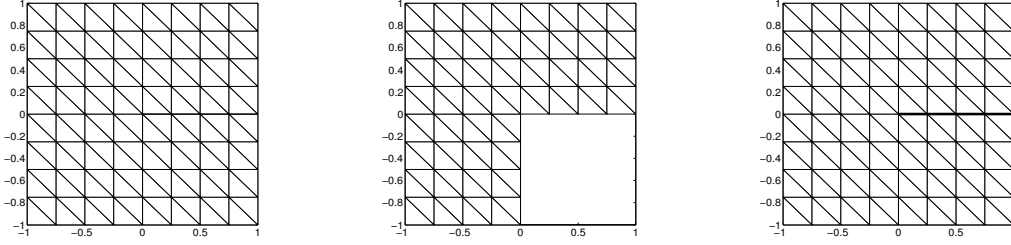
FIG. 6.1. *Typical uniform triangular meshes with* $h = 1/4$: *(left) square domain, (middle) L-shaped domain, and (right) cracked domain.*

classical for the eigenvalue problem with compact operator [6, 9, 11, 12, 57]. An intuitive observation is that in the present method, it may still provide a compact operator, by noting that the bilinear form in the method is actually $(\operatorname{curl} \boldsymbol{u}, \operatorname{curl} \boldsymbol{v}) + (R_h(\operatorname{div} \boldsymbol{u}), R_h(\operatorname{div} \boldsymbol{v}))_1 + \sum_{T \in \mathcal{T}_h} h_T^2 (\operatorname{div} \boldsymbol{u}, \operatorname{div} \boldsymbol{v})_{0,T}$. *This bilinear form is quite like the one in [37] where the eigenvalue problem is studied. However, a strict theory needs to be developed, since a method which is efficient for the source problem may not be for the eigenvalue problem [9]. For the Maxwell equations, there are many theories available. The relevant theory can be found in [11, 12, 37]. We may adapt the argument therein to the method here, but more investigations have to be further carried out.*

6. Numerical experiments. In this section, we will illustrate the high performance of the proposed mixed H^1-conforming FEM (3.1) by considering some typical examples in the literature. The numerical experiments will be divided into two parts, one for source problems and the other for eigenvalue problems. In each part, we will consider the CP_1-P_1, CP_2-P_1 and P_2-P_1 elements associated with the uniform triangulation $\mathcal{T}_h$, which is composed of uniform triangles. The uniform triangular meshes employed in the computation are drawn in Figure 6.1. Notice that for the P_2-P_1 elements, we have no convergence like Theorem 5.1 and stability like Theorem 5.2, but numerical results show that such finite elements can perform almost the same well as the CP_1-P_1 and CP_2-P_1 elements. We consider three domains: square, L-shaped domain, and cracked domain. The former two are Lipschitz domains, while the latter is not. Although theoretical results are obtained for Lipschitz domains, the numerical results show that they also hold for non-Lipschitzian cracked domain.

6.1. Source problems for Maxwell's equations. In this subsection, we consider three examples.

Example 6.1.1 (A smooth solution problem). In order to test the validity of the proposed mixed H^1-conforming FEM (3.1), we first consider Maxwell's equations on the square domain $\Omega := (-1, 1) \times (-1, 1)$, see the left part of Figure 6.1, with the smooth exact solution $\boldsymbol{u} = (u_1, u_2)$ given by

$$u_1(x, y) = \sin(2\pi y) \sin^2(\pi x), \quad u_2(x, y) = \sin(2\pi x) \sin^2(\pi y),$$

and $p(x, y) = 0$. Substituting the exact solution pair $(\boldsymbol{u}, p)$ into (2.3), we have the source terms $\boldsymbol{f}$, with div $\boldsymbol{f} = 0$, and g. We perform the proposed mixed H^1-conforming FEM (3.1) using the three different finite elements, i.e., CP_1-P_1, CP_2-P_1 and P_2-P_1 elements. The numerical results are reported in Tables 6.1–6.3.

From the numerical results we can find that for this smooth solution problem, the convergence of $\boldsymbol{u}_h$ using the CP_1-P_1 elements are second order in the L^2 norm and first order in the $H(\operatorname{curl})$ norm, while the convergence are third order in the L^2 norm and second order in the $H(\operatorname{curl})$ norm when we employ the CP_2-P_1 elements. However, the L^2 convergence rate of $\boldsymbol{u}_h$ is only two, less than the optimal order three, when we use the P_2-P_1 elements. In all these cases, the convergence rates of the dummy variable p_h are much higher than the prediction. The elevation plots of the finite element solutions with $h = 1/32$ are

TABLE 6.1
Error behavior of the smooth solution problem using CP_1-P_1 elements

$1/h$	16	32	64	128	256
$\dfrac{\|\boldsymbol{u} - \boldsymbol{u}_h\|_0}{\|\boldsymbol{u}\|_0}$	3.7489E-03	9.2910E-04	2.3157E-04	5.7825E-05	1.4424E-05
Rate	–	2.01	2.00	2.00	2.00
$\|p - p_h\|_0$	4.6464E-04	3.3096E-05	2.9421E-06	3.1971E-07	2.4014E-08
Rate	–	3.81	3.49	3.20	3.23
$\dfrac{\|\boldsymbol{u} - \boldsymbol{u}_h\|_{H(\mathrm{curl})}}{\|\boldsymbol{u}\|_{H(\mathrm{curl})}}$	4.3780E-02	2.1890E-02	1.0945E-02	5.4726E-03	2.7363E-03
Rate	–	1.00	1.00	1.00	1.00
$\|p - p_h\|_1$	7.0187E-03	9.3155E-04	1.5419E-04	2.6812E-05	3.3609E-06
Rate	–	2.91	2.59	2.52	3.00

TABLE 6.2
Error behavior of the smooth solution problem using CP_2-P_1 elements

$1/h$	16	32	64	128	256
$\dfrac{\|\boldsymbol{u} - \boldsymbol{u}_h\|_0}{\|\boldsymbol{u}\|_0}$	1.2525E-03	1.7850E-04	2.3235E-05	2.9375E-06	3.7103E-07
Rate	–	2.81	2.94	2.98	2.99
$\|p - p_h\|_0$	7.3168E-05	1.6152E-06	3.2795E-08	7.5273E-10	2.1786E-11
Rate	–	5.50	5.62	5.45	5.11
$\dfrac{\|\boldsymbol{u} - \boldsymbol{u}_h\|_{H(\mathrm{curl})}}{\|\boldsymbol{u}\|_{H(\mathrm{curl})}}$	2.9156E-03	7.0103E-04	1.7441E-04	4.3582E-05	1.0877E-05
Rate	–	2.06	2.01	2.00	2.00
$\|p - p_h\|_1$	1.1112E-03	5.4088E-05	3.2996E-06	2.0697E-07	1.3026E-08
Rate	–	4.36	4.03	3.99	3.99

given in Figures 6.2–6.4.

Example 6.1.2 (The *L*-shaped domain problem). We now consider Maxwell's equations with a non-H^1 singular solution on an *L*-shaped domain $\Omega := (-1, 1)^2 \backslash ([0, 1) \times (-1, 0])$, see the middle part of Figure 6.1. The singular solution $\boldsymbol{u}$ is given by

$$\boldsymbol{u}(x, y) = \nabla\big((1 - x^2)(1 - y^2)\varphi(x, y)\big)$$

and the multiplier p is identically equal to zero, where $x = \rho\cos\theta$, $y = \rho\sin\theta$, $\varphi(x, y) = \rho^{2/3}\sin(\frac{2}{3}\theta)$, and ρ is the distance to the origin and θ is the angular coordinate varying form 0 to $3\pi/2$. One can check that the exact solution $\boldsymbol{u}$ has a strong unbounded singularity at the origin, and it satisfies the homogeneous tangential boundary condition, $\boldsymbol{u} \cdot \boldsymbol{\tau} = 0$ on Γ. Since $\varphi \in H^{5/3-\epsilon}(\Omega)$ for any $\epsilon > 0$, it follows that $\boldsymbol{u} \in (H^{2/3-\epsilon}(\Omega))^2$ (cf. [35] and references cited therein). In other words, we have $r \approx 0.67$ in Theorem 5.1.

We now perform the mixed H^1-conforming FEM (3.1) using the CP_1-P_1, CP_2-P_1 and P_2-P_1 elements. The numerical results are reported in Tables 6.4–6.6, which support the theoretical analysis. Although many convergence rates of $\boldsymbol{u}_h$ presented in Tables 6.4–6.6 are decreasing as $h \to 0^+$, all convergence rates apparently tend to a limiting value, which is slightly higher than the theoretical estimates. Moreover, from the numerical results we can find that if the method (3.1) employs the P_2-P_1 elements, both the accuracy of $\boldsymbol{u}_h$ in the $H(\mathrm{curl})$ norm and p_h in the H^1 norm are apparently worse than the accuracy of that using CP_1-P_1 and CP_2-P_1 elements. Finally, we plot the finite element solutions using these three different finite elements

TABLE 6.3
Error behavior of the smooth solution problem using P_2-P_1 elements

$1/h$	16	32	64	128	256
$\dfrac{\|\boldsymbol{u} - \boldsymbol{u}_h\|_0}{\|\boldsymbol{u}\|_0}$	2.6553E-03	6.5576E-04	1.6343E-04	4.0827E-05	1.0205E-05
Rate	–	2.02	2.00	2.00	2.00
$\|p - p_h\|_0$	4.9886E-04	3.0360E-05	1.9076E-06	1.2300E-07	8.2867E-09
Rate	–	4.04	3.99	3.96	3.89
$\dfrac{\|\boldsymbol{u} - \boldsymbol{u}_h\|_{H(\mathrm{curl})}}{\|\boldsymbol{u}\|_{H(\mathrm{curl})}}$	7.4444E-03	1.8502E-03	4.6189E-04	1.1543E-04	2.8853E-05
Rate	–	2.01	2.00	2.00	2.00
$\|p - p_h\|_1$	5.6721E-03	4.7483E-04	8.1603E-05	1.7017E-05	3.4913E-06
Rate	–	3.58	2.54	2.26	2.29

FIG. 6.2. *Elevation plots of the CP_1-P_1 finite element solutions $\boldsymbol{u}_h = (u_{1h}, u_{2h})$ and p_h with $h = 1/32$ of the smooth solution problem.*

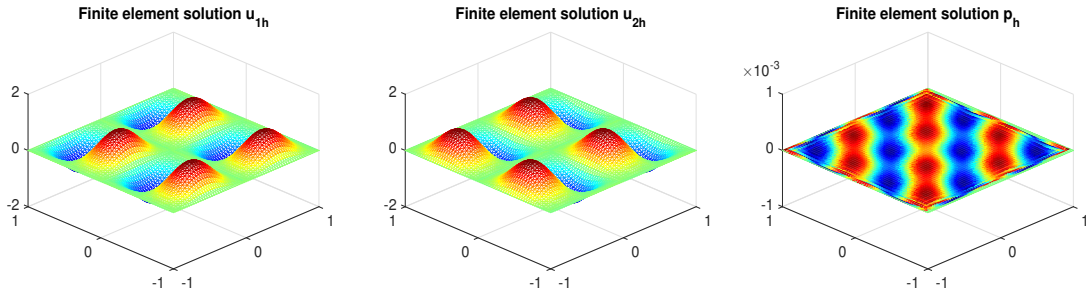FIG. 6.3. *Elevation plots of the CP_2-P_1 finite element solutions $\boldsymbol{u}_h = (u_{1h}, u_{2h})$ and p_h with $h = 1/32$ of the smooth solution problem.*

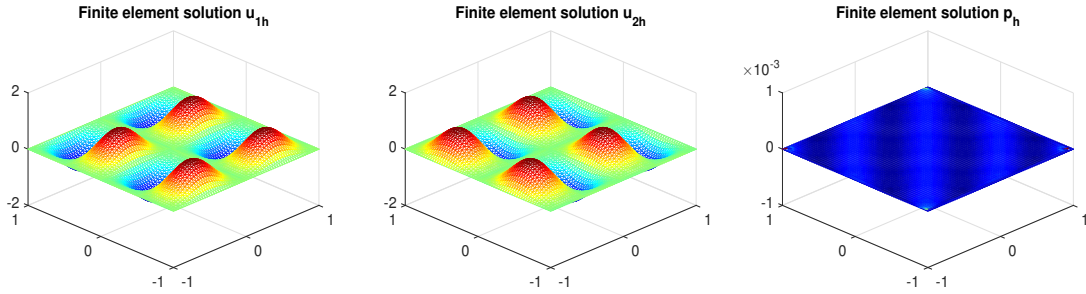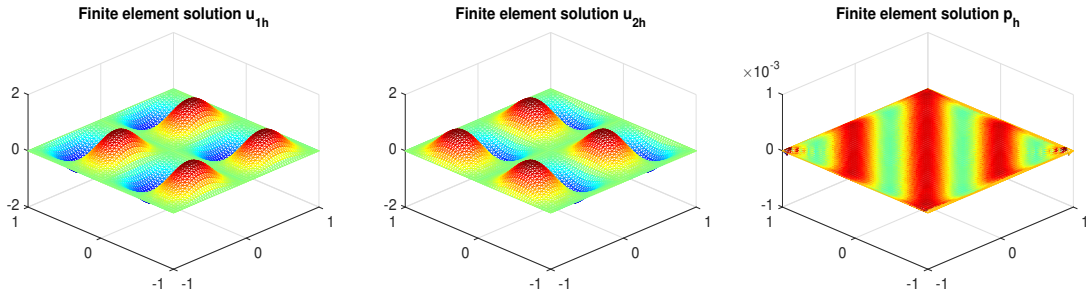FIG. 6.4. *Elevation plots of the P_2-P_1 finite element solutions $\boldsymbol{u}_h = (u_{1h}, u_{2h})$ and p_h with $h = 1/32$ of the smooth solution problem.*

TABLE 6.4
Error behavior of the L-shaped domain problem using CP_1-P_1 elements

$1/h$	16	32	64	128	256
$\dfrac{\|u - u_h\|_0}{\|u\|_0}$	3.7291E-02	1.9586E-02	1.1093E-02	6.6392E-03	4.0167E-03
Rate	—	0.93	0.82	0.74	0.72
$\|p - p_h\|_0$	2.1864E-02	9.1305E-03	3.7079E-03	1.4881E-03	5.9407E-04
Rate	—	1.26	1.30	1.32	1.32
$\dfrac{\|u - u_h\|_{H(\text{curl})}}{\|u\|_{H(\text{curl})}}$	5.3043E-02	2.4288E-02	1.2228E-02	6.8028E-03	4.0444E-03
Rate	—	1.13	0.99	0.85	0.75
$\|p - p_h\|_1$	3.5989E-01	2.3527E-01	1.5021E-01	9.5089E-02	6.0012E-02
Rate	—	0.61	0.65	0.66	0.66

TABLE 6.5
Error behavior of the L-shaped domain problem using CP_2-P_1 elements

$1/h$	16	32	64	128	256
$\dfrac{\|u - u_h\|_0}{\|u\|_0}$	2.8975E-02	1.6281E-02	9.6914E-03	5.9559E-03	3.7139E-03
Rate	—	0.83	0.75	0.70	0.68
$\|p - p_h\|_0$	1.3943E-02	5.8502E-03	2.3879E-03	9.6222E-04	3.8520E-04
Rate	—	1.25	1.29	1.31	1.32
$\dfrac{\|u - u_h\|_{H(\text{curl})}}{\|u\|_{H(\text{curl})}}$	3.6256E-02	1.7115E-02	8.9772E-03	5.1533E-03	3.1161E-03
Rate	—	1.08	0.93	0.80	0.73
$\|p - p_h\|_1$	1.8779E-01	1.2100E-01	7.6870E-02	4.8579E-02	3.0640E-02
Rate	—	0.63	0.65	0.66	0.66

with $h = 1/32$ in Figures 6.5–6.7.

Example 6.1.3 (The cracked domain problem). In this example, we take a cracked domain which is defined as $\Omega := (-1,1)^2 \backslash \{(x,y) \in \mathbb{R}^2 | \ 0 \leq x < 1, y = 0\}$, see the right part of Figure 6.1, and choose the exact solution u to be

$$u(x,y) = \nabla\big((1 - x^2)(1 - y^2)\varphi(x,y)\big)$$

and the multiplier p is identically equal to zero, where $\varphi(x,y) = \rho^{1/2} \sin(\frac{1}{2}\theta)$ and θ is varying form 0 to 2π. In this case, since $\varphi \in H^{3/2-\epsilon}(\Omega)$ for any $\epsilon > 0$, we have $u \in (H^{1/2-\epsilon}(\Omega))^2$ (cf. [35] and references cited therein). That is, we have $r \approx 0.5$ in Theorem 5.1.

Numerical results of the proposed method (3.1) using CP_1-P_1, CP_2-P_1 and P_2-P_1 elements are collected in Tables 6.7–6.9 and Figures 6.8–6.10, which support the theoretical analysis for the CP_1-P_1 and CP_2-P_1 elements, both with convergence rates higher than the predicted value 0.5; unexpectedly, P_2-P_1 element also exhibits almost the same convergence rate for u.

6.2. Eigenvalue problems for Maxwell's equations. In this subsection, we consider the Maxwell eigenvalue problem which can be posed as follows: find $\omega^2 \in \mathbb{R}$ and $u \neq 0$ such that

$$\textbf{curl}\,\text{curl}\,u = \omega^2 u, \quad \text{div}\,u = 0 \quad \text{in } \Omega, \quad u \cdot \tau = 0 \quad \text{on } \Gamma.$$

TABLE 6.6
Error behavior of the L-shaped domain problem using P_2-P_1 elements

$1/h$	16	32	64	128	256
$\dfrac{\|u - u_h\|_0}{\|u\|_0}$	3.0874E-02	1.6989E-02	9.8638E-03	5.9899E-03	3.6872E-03
Rate	—	0.86	0.78	0.72	0.70
$\|p - p_h\|_0$	2.0037E-02	9.4706E-03	4.2856E-03	1.8732E-03	8.0413E-04
Rate	—	1.08	1.14	1.19	1.22
$\dfrac{\|u - u_h\|_{H(\mathrm{curl})}}{\|u\|_{H(\mathrm{curl})}}$	6.5406E-02	3.8450E-02	2.2340E-02	1.2944E-02	7.4861E-03
Rate	—	0.77	0.78	0.79	0.79
$\|p - p_h\|_1$	2.8144E-01	2.6557E-01	2.4083E-01	2.0707E-01	1.6703E-01
Rate	—	0.08	0.14	0.22	0.31

FIG. 6.5. *Elevation plots of the CP_1-P_1 finite element solutions $u_h = (u_{1h}, u_{2h})$ and p_h with $h = 1/32$ of the L-shaped domain problem.*

FIG. 6.6. *Elevation plots of the CP_2-P_1 finite element solutions $u_h = (u_{1h}, u_{2h})$ and p_h with $h = 1/32$ of the L-shaped domain problem.*

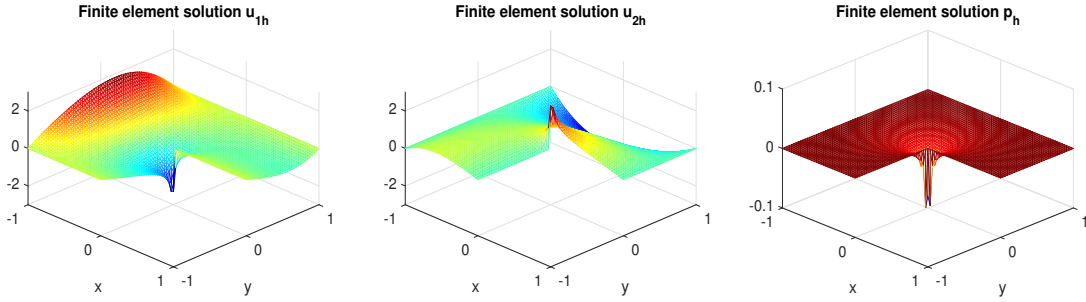
FIG. 6.7. *Elevation plots of the P_2-P_1 finite element solutions $u_h = (u_{1h}, u_{2h})$ and p_h with $h = 1/32$ of the L-shaped domain problem.*

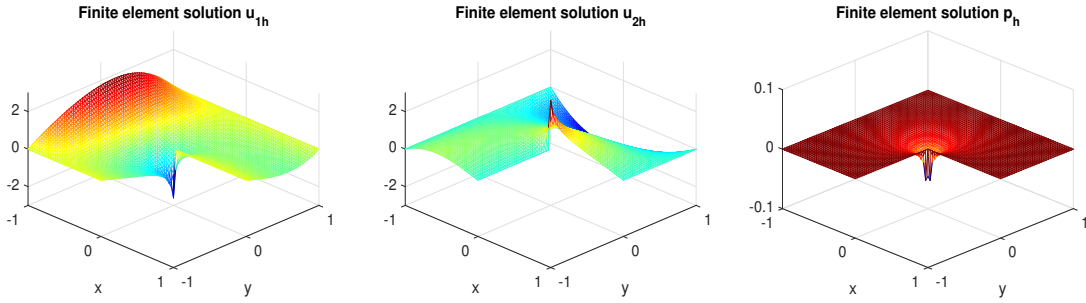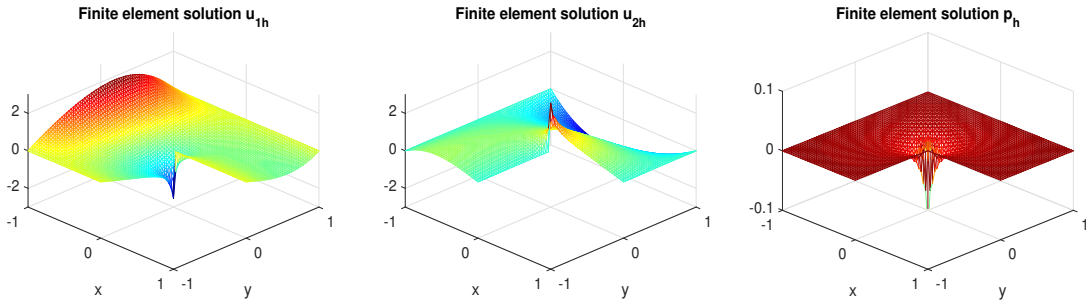TABLE 6.7
Error behavior of the cracked domain problem using CP_1-P_1 elements

$1/h$	16	32	64	128	256
$\dfrac{\\|u - u_h\\|_0}{\\|u\\|_0}$	3.0383E-01	2.0086E-01	1.2162E-01	7.0411E-02	4.1290E-02
Rate	$-$	0.60	0.72	0.79	0.77
$\\|p - p_h\\|_0$	1.7499E-01	1.1456E-01	6.7483E-02	3.6999E-02	1.9419E-02
Rate	$-$	0.61	0.76	0.87	0.93
$\dfrac{\\|u - u_h\\|_{H(\mathrm{curl})}}{\\|u\\|_{H(\mathrm{curl})}}$	4.3995E-01	2.8772E-01	1.7134E-01	9.6502E-02	5.3910E-02
Rate	$-$	0.61	0.75	0.83	0.84
$\\|p - p_h\\|_1$	1.4547E+00	1.3524E+00	1.1279E+00	8.7478E-01	6.6296E-01
Rate	$-$	0.11	0.26	0.37	0.40

TABLE 6.8
Error behavior of the cracked domain problem using CP_2-P_1 elements

$1/h$	16	32	64	128	256
$\dfrac{\\|u - u_h\\|_0}{\\|u\\|_0}$	2.5677E-01	1.6279E-01	9.6385E-02	5.5772E-02	3.2798E-02
Rate	$-$	0.66	0.76	0.79	0.77
$\\|p - p_h\\|_0$	1.4400E-01	9.0576E-02	5.1721E-02	2.7799E-02	1.4436E-02
Rate	$-$	0.67	0.81	0.90	0.95
$\dfrac{\\|u - u_h\\|_{H(\mathrm{curl})}}{\\|u\\|_{H(\mathrm{curl})}}$	3.6847E-01	2.3034E-01	1.3329E-01	7.4336E-02	4.1458E-02
Rate	$-$	0.68	0.79	0.84	0.84
$\\|p - p_h\\|_1$	1.6020E+00	1.4161E+00	1.1397E+00	8.6479E-01	6.3452E-01
Rate	$-$	0.18	0.31	0.40	0.45

Introducing the dummy variable p, the above eigenvalue problem can be put into the following mixed form

$$\mathbf{curl}\,\mathrm{curl}\,u + \nabla p = \omega^2 u, \quad \mathrm{div}\,u = 0 \quad \text{in } \Omega, \quad u \cdot \tau = 0, \quad p = 0 \quad \text{on } \Gamma,$$

and the variational problem reads: find $\omega^2 \in \mathbb{R}$ and $0 \neq u \in H_0(\mathrm{curl}; \Omega)$, $p \in H_0^1(\Omega)$ such that

$$(\mathrm{curl}\,u, \mathrm{curl}\,v) + (\nabla p, v) + (u, \nabla q) = \omega^2(u, v) \quad \forall\, v \in H_0(\mathrm{curl}; \Omega), \ \forall\, q \in H_0^1(\Omega).$$

The mixed H^1-conforming stabilized FEM is then formulated as: find $\omega_h^2 \in \mathbb{R}$ and $0 \neq u_h \in U_h$, $p_h \in Q_h$ such that

$$(\mathrm{curl}\,u_h, \mathrm{curl}\,v_h) + \sum_{T \in \mathcal{T}_h} h_T^2 (\mathrm{div}\,u_h, \mathrm{div}\,v_h)_{0,T} + (\nabla p_h, v_h) + (u_h, \nabla q_h)$$

$$= \omega_h^2(u_h, v_h) \quad \forall\, v_h \in U_h, \ \forall\, q_h \in Q_h.$$

We first consider the eigenvalue problem on the L-shaped domain $\Omega := (-1,1)^2 \setminus ([0,1] \times (-1,0])$. We will take the nonzero eigenvalues provided by Monique Dauge at her personal webpage

http://perso.univ-rennes1.fr/monique.dauge/benchmax.html

as the benchmark. For example, the first two nonzero eigenvalues given there are

$$\omega_1^2 = 1.47562182408 \quad \text{and} \quad \omega_2^2 = 3.53403136678.$$

TABLE 6.9
Error behavior of the cracked domain problem using P_2-P_1 elements

$1/h$	16	32	64	128	256
$\dfrac{\\|u - u_h\\|_0}{\\|u\\|_0}$	3.4891E-01	2.7031E-01	1.8801E-01	1.1878E-01	7.0781E-02
Rate	–	0.37	0.52	0.66	0.75
$\\|p - p_h\\|_0$	2.0740E-01	1.6185E-01	1.1152E-01	6.8533E-02	3.8660E-02
Rate	–	0.36	0.54	0.70	0.83
$\dfrac{\\|u - u_h\\|_{H(\mathrm{curl})}}{\\|u\\|_{H(\mathrm{curl})}}$	5.2711E-01	4.0705E-01	2.8046E-01	1.7416E-01	1.0075E-01
Rate		0.37	0.54	0.69	0.79
$\\|p - p_h\\|_1$	3.9209E+00	5.9934E+00	8.2002E+00	1.0050E+01	1.1324E+01
Rate	–	-0.61	-0.45	-0.29	-0.17

FIG. 6.8. *Elevation plots of the CP_1-P_1 finite element solutions $u_h = (u_{1h}, u_{2h})$ and p_h with $h = 1/32$ of the cracked domain problem.*

FIG. 6.9. *Elevation plots of the CP_2-P_1 finite element solutions $u_h = (u_{1h}, u_{2h})$ and p_h with $h = 1/32$ of the cracked domain problem.*
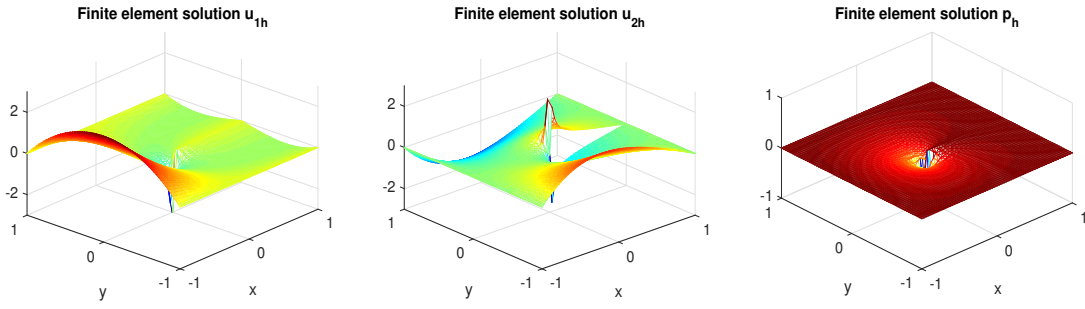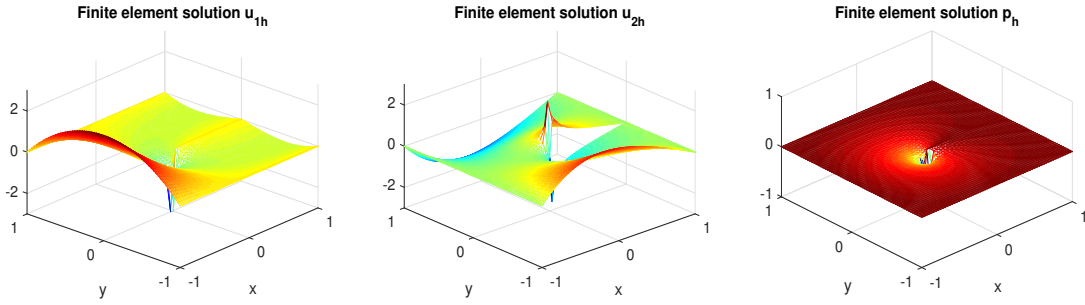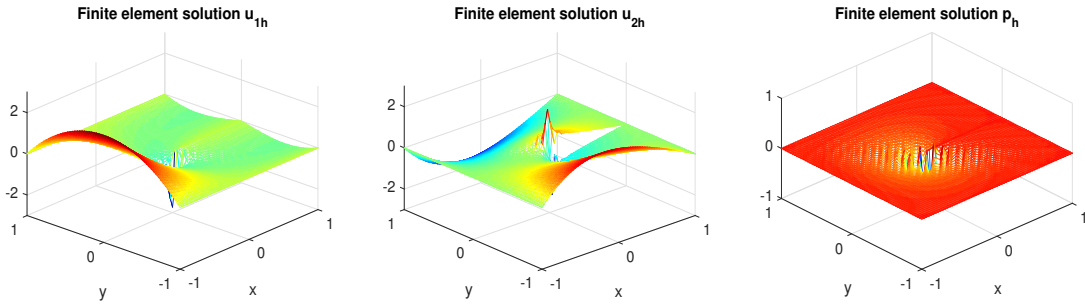

FIG. 6.10. *Elevation plots of the P_2-P_1 finite element solutions $u_h = (u_{1h}, u_{2h})$ and p_h with $h = 1/32$ of the cracked domain problem.*

TABLE 6.10
Relative errors of the eigenvalues of the L-shaped domain problem using CP_1-P_1 elements

ω^2	$1/h$	ω_h^2	$|\omega^2 - \omega_h^2|/|\omega^2|$	Rate
	16	1.94500948373	3.1809E-01	—
	32	1.67437602654	1.3469E-01	1.24
1.47562182408	64	1.55659198774	5.4872E-02	1.30
	128	1.50809033821	2.2003E-02	1.32
	256	1.48855985029	8.7678E-03	1.33
	16	3.53798759701	1.1195E-03	—
	32	3.53473810678	1.9998E-04	2.48
3.53403136678	64	3.53416098758	3.6678E-05	2.45
	128	3.53405625089	7.0413E-06	2.38
	256	3.53403639898	1.4239E-06	2.31

TABLE 6.11
Relative errors of the eigenvalues of the L-shaped domain problem using CP_2-P_1 elements

ω^2	$1/h$	ω_h^2	$|\omega^2 - \omega_h^2|/|\omega^2|$	Rate
	16	1.77285558616	2.0143E-01	—
	32	1.59849880463	8.3271E-02	1.27
1.47562182408	64	1.52518554833	3.3588E-02	1.31
	128	1.49541776405	1.3415E-02	1.32
	256	1.48349772085	5.3373E-03	1.33
	16	3.53530808872	3.6127E-04	—
	32	3.53423550577	5.7764E-05	2.64
3.53403136678	64	3.53406364542	9.1337E-06	2.66
	128	3.53403645567	1.4400E-06	2.67
	256	3.53403216843	2.2684E-07	2.67

The corresponding eigenfunctions are $\mathbf{u}^1 \in (H^{2/3-\epsilon}(\Omega))^2$ and $\mathbf{u}^2 \in (H^{4/3-\epsilon}(\Omega))^2$, for any $\epsilon > 0$ (cf. [29]). we remark that the convergence rate of the nonzero finite element eigenvalue ω_h^2 to ω^2 is depending on the regularity of the associated eigenfunction $\boldsymbol{u}$ and the degree of the finite elements employed. The numerical results of the CP_1-P_1, CP_2-P_1 and P_2-P_1 elements are presented in Tables 6.10–6.12. One can find that our method can approximate the eigenvalues very well, consistent with Remark 5.5. Moreover, we can accurately approximate the other three nonzero eigenvalues given by Monique Dauge as well.

Next, we consider the eigenvalue problem on the cracked domain $\Omega := (-1,1)^2 \setminus \{(x,y) \in \mathbb{R}^2| \ 0 \leq x < 1, y = 0\}$. Again, we take the first four nonzero eigenvalues from Monique Dauge's webpage as the benchmark as follows:

$$\omega_1^2 = 1.03407400850, \quad \omega_2^2 = 2.46740110027, \quad \omega_3^2 = 4.04692529140, \quad \omega_4^2 = 9.86960440109.$$

Note that the second and fourth eigenvalues are $\pi^2/4$ and π^2 respectively, whose eigenfunctions are smooth analytical functions. The corresponding eigenfunctions are given by $\boldsymbol{u}^1 \in (H^{1/2-\epsilon}(\Omega))^2$ for any $\epsilon > 0$ and $\boldsymbol{u}^2, \boldsymbol{u}^4 \in (H^1(\Omega))^2$. The regularity of $\boldsymbol{u}^3$ is not known, but our numerical results show that $\boldsymbol{u}^3 \in (H^{3/2-\epsilon}(\Omega))^2$. Numerical results of the CP_1-P_1, CP_2-P_1 and P_2-P_1 elements are reported in Tables 6.13–6.15. We remark that we can also accurately approximate the other six nonzero eigenvalues given by Monique Dauge.

We also note that there are somewhat different convergent behaviours between the L-shaped domain and the cracked domain. But, so far, the reason is not known.

TABLE 6.12

Relative errors of the eigenvalues of the L-shaped domain problem using P_2-P_1 elements

ω^2	$1/h$	ω_h^2	$|\omega^2 - \omega_h^2|/|\omega^2|$	Rate
	16	2.10697896768	4.2786E-01	—
	32	1.76373963076	1.9525E-01	1.13
1.47562182408	64	1.59714914007	8.2357E-02	1.25
	128	1.52507568731	3.3514E-02	1.30
	256	1.49544665026	1.3435E-02	1.32
	16	3.53919639898	1.4615E-03	—
	32	3.53492549776	2.5301E-04	2.53
3.53403136678	64	3.53417588022	4.0892E-05	2.63
	128	3.53405428048	6.4837E-06	2.66
	256	3.53403498178	1.0229E-06	2.66

TABLE 6.13

Relative errors of the eigenvalues of the cracked domain problem using CP_1-P_1 elements

ω^2	$1/h$	ω_h^2	$|\omega^2 - \omega_h^2|/|\omega^2|$	Rate
	16	2.28295406910	1.2077E+00	—
1.03407400850	32	1.71321531554	6.5676E-01	0.88
	64	1.38849238184	3.4274E-01	0.94
	128	1.21514601176	1.7511E-01	0.97
	16	2.46771253012	1.2622E-04	—
2.46740110027	32	2.46747809341	3.1204E-05	2.02
	64	2.46742029475	7.7792E-06	2.00
	128	2.46740589552	1.9434E-06	2.00
	16	4.04851577464	3.9301E-04	—
4.04692529140	32	4.04722883713	7.5007E-05	2.39
	64	4.04698906500	1.5759E-05	2.25
	128	4.04693971174	3.5633E-06	2.14
	16	9.87458325214	5.0446E-04	—
9.86960440109	32	9.87083605716	1.2479E-04	2.02
	64	9.86991149812	3.1115E-05	2.00
	128	9.86968112436	7.7737E-06	2.00

7. Concluding remarks. In this paper, we have proposed a mixed H^1-conforming FEM for solving Maxwell's equations in the vector potential form with non-H^1 singular solutions. The occurrence of singular solution is mainly due to the non-convex physical domain with reentrant corners or edges, and this causes many difficulties for numerical solution. The Maxwell equations is formulated in terms of electric field and Lagrange multiplier, where the multiplier is additionally introduced accounting for the divergence constraint. We have provided a general framework of stability and error analysis for the proposed mixed H^1-conforming FEM by verifying the $\mathcal{K}_h$-coercivity and the Babuška-Brezzi inf-sup condition. We have analyzed a specific pair of H^1-conforming finite elements, namely the CP_2-P_1 elements, for electric field and multiplier, and have also established the stability and error bounds of the mixed finite element solutions. To illustrate the high performance of the proposed FEM, we have presented some numerical experiments for source problems as well as eigenvalue problems on L-shaped and cracked domains. The numerical results confirm the theoretical estimates. Finally, we remark that the proposed mixed H^1-conforming FEM can be applied to solving Maxwell's equations in 3D with non-H^1 singular solutions as well. Similar Clough-Tocher and Powell-Sabin refinements in 3D are available, see, e.g., [4, 47, 51, 53], and the regular-singular decompositions similar to (5.3) may be found in [27, 28].

TABLE 6.14
Relative errors of the eigenvalues of the cracked domain problem using CP$_2$-P$_1$ elements

ω^2	$1/h$	ω_h^2	$\|\omega^2 - \omega_h^2\|/\|\omega^2\|$	Rate
1.03407400850	16	1.89476337739	8.3233E-01	—
	32	1.48919574044	4.4012E-01	0.92
	64	1.26819358462	2.2641E-01	0.96
	128	1.15282009449	1.1483E-01	0.98
2.46740110027	16	2.46740118334	3.3667E-08	—
	32	2.46740110522	2.0082E-09	4.07
	64	2.46740110058	1.2641E-10	3.99
	128	2.46740110027	5.2735E-14	11.23
4.04692529140	16	4.04720868130	7.0026E-05	—
	32	4.04696134468	8.9088E-06	2.97
	64	4.04692981875	1.1187E-06	2.99
	128	4.04692585796	1.4000E-07	3.00
9.86960440109	16	9.86960969039	5.3592E-07	—
	32	9.86960471776	3.2086E-08	4.06
	64	9.86960442060	1.9764E-09	4.02
	128	9.86960440228	1.2051E-10	4.04

TABLE 6.15
Relative errors of the eigenvalues of the cracked domain problem using P$_2$-P$_1$ elements

ω^2	$1/h$	ω_h^2	$\|\omega^2 - \omega_h^2\|/\|\omega^2\|$	Rate
1.03407400850	16	2.87805387607	1.7832E+00	—
	32	2.16440461011	1.0931E+00	0.71
	64	1.66910377875	6.1410E-01	0.83
	128	1.37213197183	3.2692E-01	0.91
2.46740110027	16	2.46740129336	7.8257E-08	—
	32	2.46740111224	4.8529E-09	4.01
	64	2.46740110102	3.0448E-10	3.99
	128	2.46740110033	2.3008E-11	3.73
4.04692529140	16	4.04833330870	3.4792E-04	—
	32	4.04712863043	5.0245E-05	2.79
	64	4.04695179961	6.5502E-06	2.94
	128	4.04692864450	8.2856E-07	2.98
9.86960440109	16	9.86961672238	1.2484E-06	—
	32	9.86960516667	7.7569E-08	4.01
	64	9.86960444887	4.8407E-09	4.00
	128	9.86960440408	3.0324E-10	4.00

Appendix. In this section, the proof for the error estimate (5.17) is given.

PROPOSITION A.1. *Let $\boldsymbol{u}$ be given by (5.3). Assume that $\boldsymbol{u} \in (H^r(\Omega))^2$ for some $r > 1/2$. Additionally, assume that $\mathrm{div}\,\boldsymbol{u} \in L^2(\Omega)$. Let $\tilde{\boldsymbol{u}}_h \in U_h$ be given by (5.10). Then,*

$$\sum_{T \in \mathcal{T}_h} h_T^2 \|\mathrm{div}\,(\boldsymbol{u} - \tilde{\boldsymbol{u}}_h)\|_{0,T}^2 \leq Ch^{2r}\left(\|\boldsymbol{u}^R\|_{1+r}^2 + \|p^S\|_{1+r}^2 + \|\mathrm{div}\,\boldsymbol{u}\|_0^2\right).$$

Proof. We first introduce the nonconforming linear element [31] and recall the finite element interpolation properties. Introduce

$$V_h = \left\{ v \in (L^2(\Omega))^2 : v|_T \in (P_1(T))^2, \forall\, T \in \mathcal{T}_h, v \text{ continuous at all mid-points of element} \right.$$
$$\left. \text{boundaries in } \Omega, v \cdot \tau = 0 \text{ at all mid-points of element boundaries on } \Gamma \right\}.$$

Let $J_h u \in V_h$ denote the finite element interpolation of u in V_h, which is defined by

$$\int_F J_h u = \int_F u \quad \forall\, F \subset \partial T, \forall\, T \in \mathcal{T}_h.$$

Let ρ_h denote the piecewise constant L^2 projection operator, i.e., given a $\chi \in L^2(\Omega)$, $\rho_h \chi|_T = \int_T \chi / |T|$ for all $T \in \mathcal{T}_h$, where $|T|$ is the area of T. We have for all $T \in \mathcal{T}_h$,

$$\text{curl}\, (J_h u|_T) = (\rho_h \text{curl}\, u)_T, \quad \text{div}\, (J_h u|_T) = (\rho_h \text{div}\, u)|_T, \quad \|u - J_h u\|_0 \leq Ch^r\|u\|_r,$$
$$\|\text{curl}\, (u - J_h u)\|_{0,T} \leq 2\|\text{curl}\, u\|_{0,T}, \quad \|\text{div}\, (u - J_h u)\|_{0,T} \leq 2\|\text{div}\, u\|_{0,T}.$$

By the triangle inequality, inverse estimates in [21], we have

$$h_T^2\|\text{div}\, (u - \tilde{u}_h)\|_{0,T}^2 \leq 2h_T^2\big(\|\text{div}\, (u - J_h u)\|_{0,T}^2 + \|\text{div}\, (J_h u - \tilde{u}_h)\|_{0,T}^2\big)$$
$$\leq 8h_T^2\|\text{div}\, u\|_{0,T}^2 + 2h_T^2\|\text{div}\, (\tilde{u}_h - J_h u)\|_{0,T}^2$$
$$\leq 8h_T^2\|\text{div}\, u\|_{0,T}^2 + C\|\tilde{u}_h - J_h u\|_{0,T}^2$$
$$\leq 8h_T^2\|\text{div}\, u\|_{0,T}^2 + C\|\tilde{u}_h - u\|_{0,T}^2 + C\|u - J_h u\|_{0,T}^2.$$

Summing over $\mathcal{T}_h$, the conclusion follows, by noting (5.11) and $\|u - J_h u\|_0 \leq Ch^r\|u\|_r$ and that from (5.3), we have $\|u\|_r \leq C(\|u^R\|_{1+r} + \|p^S\|_{1+r})$. □

REFERENCES

[1] C. Amrouche, C. Bernardi, M. Dauge, and V. Girault, Vector potentials in three-dimensional non-smooth domains, *Math. Methods Appl. Sci.,* 21 (1998), pp. 823-864.
[2] F. Assous, P. Ciarlet, Jr., P.-A. Ravairt, and E. Sonnendrücker, Characterization of the singular part of the solution of Maxwell's equations in a polyhedral domain, *Math. Methods Appl. Sci.,* 22 (1999), pp. 485-499.
[3] F. Assous, P. Ciarlet, Jr., and E. Sonnendrücker, Resolution of the Maxwell equations in a domain with reentrant corners, *ESAIM-Math. Model. Numer. Anal.,* 32 (1998), pp. 359-389.
[4] G. Awanou and M.-J. Lai, C^1 quintic spline interpolation over tetrahedral partitions, in: *Approximation Theory X: Wavelets, Splines, and Applications,* C. K. Chui, L. L. Schumaker, and J. Stoeckler, eds., Vanderbilt University Press, 2002, pp. 1-16.
[5] G. Awanou and M.-J. Lai, Trivariate spline approximations of 3D Navier-Stokes equations, *Math. Comput.,* 74 (2004), pp. 585-601.
[6] I. Babuška and J. Osborn, Eigenvalue problems, in: *Handbook of Numerical Analysis, Vol. II, Finite Element Methods (part 1),* P. G. Ciarlet and J. L. Lions, eds., North-Holland, Amsterdam, 1991, pp. 641-787.
[7] S. Badia and R. Codina, A nodal-based finite element approximation of the Maxwell problem suitable for singular solutions, *SIAM J. Numer. Anal.,* 50 (2012), pp. 398-417.
[8] M. Bercovier and O. Pironneau, Error estimates for finite element solution of the Stokes problem in the primitive variables, *Numer. Math.,* 33 (1979), pp. 211-224.
[9] D. Boffi, Finite element approximation of eigenvalue problems, *Acta Numerica,* (2010), pp. 1-120.
[10] D. Boffi, P. Fernandes, L. Gastaldi, and I. Perugia, Computational models of electromagnetic resonators: analysis of edge element approximation, *SIAM J. Numer. Anal.,* 36 (1999), pp. 1264-1290.
[11] A. Bonito and J.-L. Guermond, Approximation of the eigenvalue problem for the time-harmonic Maxwell system by continuous Lagrange finite elements, *Math. Comput.,* 80 (2011), pp. 1887-1910.
[12] A. Bonito, J.-L. Guermond, and F. Luddens, An interior penalty method with C^0 finite elements for the approximation of the Maxwell equations in heterogeneous media: convergence analysis with minimal regularity, *ESAIM-Math. Model. Numer. Anal.,* 50 (2016), pp. 1457-1489.

[13] A. Bossavit, *Computational Electromagnetism: Variational Formulations, Complementarity, Edge Elements,* Academic Press, San Diego, 1998.

[14] J. H. Bramble, T. V. Kolev, and J. E. Pasciak, The approximation of the Maxwell eigenvalue problem using a least-squares method, *Math. Comput.,* 74 (2005), pp.1575-1598.

[15] J. H. Bramble and J. E. Pasciak, A new approximation technique for div-curl systems, *Math. Comput.,* 73 (2003), pp. 1739-1762.

[16] S. C. Brenner and L. R. Scott, *The Mathematical Theory of Finite Element Methods,* Springer-Verlag, Berlin, 1996.

[17] F. Brezzi and M. Fortin, *Mixed and Hybrid Finite Element Methods,* Springer-Verlag, New York, 1991.

[18] A. Buffa, P. Ciarlet, Jr., and E. Jamelot, Solving electromagnetic eigenvalue problems in polyhedral domains with nodal finite elements, *Numer. Math.,* 113 (2009), pp. 497-518.

[19] M. Cessenat, *Mathematical Methods in Electromagnetism: Linear Theory and Applications,* World Scientific, Singapore, 1996.

[20] P. G. Ciarlet, *The Finite Element Method for Elliptic Problems,* North-Holland, Amsterdam, 1978.

[21] P. G. Ciarlet, Basic error estimates for elliptic problems, in: *Handbook of Numerical Analysis, Vol. II, Finite Element Methods (part 1),* P. G. Ciarlet and J. L. Lions, eds., North-Holland, Amsterdam, 1991, pp. 17-351.

[22] P. Ciarlet, Jr. and V. Girault, Inf-sup condition for the 3-D P_2-iso-P_1 Taylor-Hood finite element; application to Maxwell equations, *C. R. Acad. Sci. Paris, Ser. I,* 335 (2002), pp. 827-832.

[23] P. Ciarlet, Jr. and S. Labrunie, Numerical analysis of the generalized Maxwell equations (with an elliptic correction) for charged particle simulations, *Math. Models Methods Appl. Sci.,* 19 (2009), pp. 1959-1994.

[24] P. Ciarlet, Jr., F. Lefèvre, S. Lohrengel, and S. Nicaise, Weighted regularization for composite materials in electromagnetism, *ESAIM-Math. Model. Numer. Anal.,* 44 (2010), pp. 75-108.

[25] P. Ciarlet, Jr. and J. Zou, Fully discrete finite element approaches for time-dependent Maxwell's equations, *Numer. Math.,* 82 (1999), pp. 193-219.

[26] M. Costabel, A remark on the regularity of solutions of Maxwell's equations on Lipschitz domains, *Math. Methods Appl. Sci.,* 12 (1990), pp. 365-368.

[27] M. Costabel and M. Dauge, Singularities of electromagnetic fields in polyhedral domains, *Arch. Rational Mech. Anal.,* 151 (2000), pp. 221-276.

[28] M. Costabel and M. Dauge, Weighted regularization of Maxwell equations in polyhedral domains, *Numer. Math.,* 93 (2002), pp. 239-277.

[29] M. Costabel and M. Dauge, Computation of resonance frequencies for Maxwell equations in non-smooth domains, in: *Lecture Notes in Computational Science and Engineering, Vol. 31,* M. Ainsworth, P. Davies, D. Duncan, P. Martin, and B. Rynne, eds., Springer-Verlag, Berlin, 2003, pp. 125-161.

[30] M. Costabel, M. Dauge, and S. Nicaise, Singularities of Maxwell interface problems, *ESAIM-Math. Model. Numer. Anal.,* 33 (1999), pp. 627-649.

[31] M. Crouzeix and P.-A. Raviart, Conforming and nonconforming finite element methods for solving the stationary Stokes equations, *RAIRO Numer. Anal.,* 7 (1973), pp. 33-75.

[32] H. Y. Duan, F. Jia, P. Lin, and R. C. E. Tan, The local L^2 projected C^0 finite element method for Maxwell problem, *SIAM J. Numer. Anal.,* 47 (2009), pp. 1274-1303.

[33] H. Y. Duan, S. Li, R. C. E. Tan, and W. Y. Zheng, A delta-regularization finite element method for a double curl problem with divergence-free constraint, *SIAM J. Numer. Anal.,* 50 (2012), pp. 3208-3230.

[34] H. Y. Duan, P. Lin, P. Saikrishnan, and R. C. E. Tan, A least squares finite element method for the magnetostatic problem in a multiply-connected Lipschitz domain, *SIAM J. Numer. Anal.,* 45 (2007), pp. 2537-2563.

[35] H. Y. Duan, P. Lin, and R. C. E. Tan, C^0 elements for generalized indefinite Maxwell's equations, *Numer. Math.,* 122 (2012), pp. 61-99.

[36] H. Y. Duan, P. Lin, and R. C. E. Tan, Analysis of a continuous finite element method for $H(\mathrm{curl}, \mathrm{div})$-elliptic interface problem, *Numer. Math.,* 123 (2013), pp. 671-707.

[37] H. Y. Duan, P. Lin, and R. C. E. Tan, Error estimates for a vectorial second-order elliptic eigenproblem by the local L^2 projected C^0 finite element method, *SIAM J. Numer. Anal.,* 51 (2013), pp. 1678-1714.

[38] H. Y. Duan, R. C. E. Tan, S.-Y. Yang, and C.-S. You, Computation of Maxwell singular solution by nodal-continuous elements, *J. Comput. Phys.,* 268 (2014), pp. 63-83.

[39] R. S. Falk, A Fortin operator for two-dimensional Taylor-Hood elements, *ESAIM-Math. Model. Numer. Anal.,* 42 (2008), pp 411-424.

[40] P. Fernandes and G. Gilardi, Magnetostatic and electrostatic problems in inhomogeneous anisotropic media with irregular boundary and mixed boundary conditions, *Math. Models and Methods Appl. Sci.,* 7 (1997), pp. 957-991.

[41] P. Fernandes and I. Perugia, Vector potential formulation for magnetostatics and modelling of permanent magnets, *IMA J. Appl. Math.,* 66 (2001), pp. 293-318.

[42] M. S. Floater and M.-J. Lai, Polygonal spline spaces and the numerical solution of the Poisson equation, *SIAM J. Num. Anal.,* 54 (2016), pp. 797-824.

[43] V. Girault and P.-A. Raviart, *Finite Element Methods for Navier-Stokes Equations: Theory and Algorithms,* Springer-Verlag, Berlin, 1986.

[44] R. Hiptmair, Finite elements in computational electromagnetism, *Acta Numerica,* 11 (2002), pp. 237-339.

[45] B.-N. Jiang, *The Least-Squares Finite Element Method,* Springer-Verlag, New York, 1998.

[46] J.-M. Jin, *The Finite Element Method in Electromagnetics, 2nd Edition,* John Wiley & Sons, New York, 2002.

[47] M.-J. Lai and A. LeMehaute, A new kind of trivariate C^1 spline space, *Adv. Comput. Math.,* 21 (2004), pp. 273-292.

[48] M.-J. Lai, C. Liu, and P. Wenston, Bivariate spline method for numerical solution of time evolution Navier-Stokes equations over polygons in stream function formulation, *Numer. Methods Partial Differential Eq.,* 19 (2003), pp. 776-827.

[49] M.-J. Lai and M. Matt, A C^r trivariate macro-element based on Alfeld split, *J. Appr. Theo.,* 175 (2013), pp. 114-131.

[50] M.-J. Lai and L. L. Schumaker, Macro-elements and stable local bases for splines on Powell-Sabin triangulations, *Math. Comput.,* 72 (2003), pp. 335-354.

[51] M.-J. Lai and L. L. Schumaker, *Spline Functions on Triangulations,* Cambridge University Press, Cambridge, 2007.

[52] M.-J. Lai and P. Wenston, Bivariate spline method for numerical solution of Navier-Stokes equations over polygons in stream function formulation, *Numer. Methods Partial Differential Eq.,* 16 (2000), pp. 147-183.

[53] M.-J. Lai and P. Wenston, Trivariate C^1 cubic splines for numerical solution of biharmonic equations, in: *Trends in Approximation Theory,* K. Kopotun, T. Lyche, and M. Neamtu, eds., Vanderbilt University Press, 2001, pp. 224-234.

[54] E. J. Lee and T. A. Manteuffel, FOSLL* method for the eddy current problem with three-dimensional edge singularities, *SIAM J. Numer. Anal.,* 45 (2007), pp. 787-809.

[55] E. J. Lee, T. A. Manteuffel, and C. R. Westphal, Weighted-norm first-order system least-squares (FOSLS) for div/curl systems with three dimensional edge singularities, *SIAM J. Numer. Anal.,* 46 (2008), pp. 1619-1639.

[56] K.-A. Mardal, J. Schöberl, and R. Winther, A uniformly stable Fortin operator for the Taylor-Hood element, *Numer. Math.,* 123 (2013), pp. 537-551.

[57] B. Mercier, J. Osborn, J. Rappaz, and P.-A. Raviart, Eigenvalue approximation by mixed and hybrid methods, *Math. Comput.,* 36 (1981), pp. 427-453.

[58] P. Monk, *Finite Element Methods for Maxwell's Equations,* Oxford University Press, New York, 2003.